November 2019

Sandy Dredge Pit Sedimentation – Characteristics and Processes in Caminada Borrow Area, Ship Shoal, Louisiana Shelf, USA

Zehao Xue
Louisiana State University and Agricultural and Mechanical College

SANDY DREDGE PIT SEDIMENTATION – CHARACTERISTICS AND PROCESSES IN CAMINADA BORROW AREA, SHIP SHOAL, LOUISIANA SHELF, USA

A Thesis

Submitted to the Graduate Faculty of the
Louisiana State University and
Agricultural and Mechanical College
in partial fulfillment of the
requirements for the degree of
Master of Science

in

The Department of Geology and Geophysics

by
Zehao Xue
B.S., University of Texas at Austin, 2017
December 2019

Acknowledgements

First, I would like to give a special thanks to Dr. Carol Wilson for endless patience, guidance, and encouragement. I would also like to thank my committee members Dr. Samuel J. Bentley and Dr. Kehui (Kevin) Xu for valuable feedback and insight.

Thanks to Dr. Chunyan Li, Dr. Nan Walker, and Haoran Liu for providing additional data and collaboration. Thanks to LSU Coastal Studies Institute field support staff for valuable help in the field.

Finally, I would like to thank my family and friends for supporting me through the experience. Thank you, Doc, for igniting my passion in science; I hope I've made you proud.

Funding for this study was provided by the U.S. Department of the Interior, Bureau of Ocean Energy Management, Coastal Marine Institute, Washington DC, under Cooperative Agreement Number M16AC00018 and M17AC00019.

Table of Contents

Abstract

Mississippi River Deltaic Plain's barrier islands are undergoing rapid disintegration due to high rates of subsidence and a deficit in coastal sediment supply. To mitigate for barrier island land loss, Louisiana has implemented a restoration program that supplements coastal sediment deficits by introducing sand from outside of the active coastal system. Ship Shoal is an inner-shelf submarine shoal with large amounts of restoration quality sand that was dredged in 2013-2016 for the Caminada Headland Restoration Project in central Louisiana, USA.

Vibracore samples (1.5 - 3.5 m deep) collected in 2017 and 2018 in Caminada Borrow Area revealed new silts and clays deposited at the surface, underlain by original Ship Shoal sand and older pro-delta deposits. Through analyzing Beryllium-7 (^{7}Be) inventories in shallower multicores, we find that in 2017, 4-12 cm of sediments were deposited in Caminada Borrow Area with sedimentation rates at 0.02 – 0.06 cm/day. During repeat coring in 2018, 8-16 cm of sediments were deposited and sedimentation rates were calculated to be 0.05 – 0.15 cm/day. There is little difference in grain sizes between the two years, although interlaminated silty packages with a few isolated sand lenses can be seen in x-ray images.

Clays and fine silts deposited in Caminada Borrow Area were likely sourced from the Atchafalaya River plume during the study period, with some contribution from the main-stem Mississippi River and resuspension from ambient bays and inner shelf. Analysis of local wind/wave data revealed that Atchafalaya plume sediments extend southeastward to reach Caminada Borrow Area immediately following winter storms or tropical storms. Resuspension and redeposition during higher energy storm or hurricane events likely produced the observed coarse silt laminations. Sedimentation in the borrow area is not greatly affected by wall slope failure, evidenced by the lack of Ship Shoal sand in Caminada Borrow fill deposits. These results

are in contrast with recent studies of mud-capped dredge pits on the Louisiana continental shelf and numerical models, as infilling rate is slower than predicted and the material is mainly silts and clays. Restoration quality sand on this particular sandy shoal in Louisiana is thus not renewable.

1. Introduction

Barrier islands are sedimentary deposits that provide important protection to interior wetlands and help maintain estuarine gradients (Penland et al., 1989). Mississippi River delta plain barrier islands are undergoing rapid disintegration due to high rates of relative sea-level rise approaching ~0.9 cm/year, deficit in coastal sand supply, and erosion due to storm waves and currents (Penland and Ramsey, 1990; Miner et al., 2009; Stone and McBride, 2012; Maloney et al 2018). To mitigate for barrier island land loss, Louisiana has had a restoration program in place since 1989 that in recent years supplements coastal sediment deficits with sand from outside of the active coastal system (Van Heerden and DeRouen, 1997; Nairn et al, 2004; Kulp et al., 2005). One such technique involves using dredged sand resources from borrow areas transported to recovery sites. Kindinger et al. (2001) identified potential sand resources in Louisiana in the forms of spit platforms, delta sheet sands, ebb-tidal deltas, distributary mouth bars, distributary-channel fills, and inner shelf shoals. Of these, paleo channels—sand bodies that are former river channels—have been the subject of recent dredge operations for barrier island restoration. These sandy channel deposits have been buried by modern muddy sediment and are commonly referred to as “mud-capped” dredge pits (e.g., Peveto Channel, Raccoon Island, and Sandy Point dredged in 2003, 2013 and 2012, respectively; Obelcz et al., 2018, Fig. 1). While these dredging efforts yielded large volumes of sand (2-3 × 10^6 m^3), larger sand deposits are preferred for restoration due to its coherence (Khalil et al, 2007). Louisiana inner shelf shoals have been identified as a primary sand resource containing large volumes of restoration quality sand not covered by muddy overburden (Kulp et al., 2005). Though there have been feasibility studies on the quality of sand resources pre-dredging (Motti and Kulp, 2003; Khalil et al., 2007)

and numerical modeling for post-dredge evolution (Nairn et al., 2005), there has been little geological field study on the evolution of a sandy dredge pit and sedimentation post-dredging.

In this study, we aim to understand sandy dredge pit sedimentation and evolution through coring of Caminada Borrow Area on eastern Ship Shoal, Louisiana, dredged in 2017 (see Fig 1). Previous modeling work for coastal restoration by Nairn et al. (2005) hypothesized that a dredge pit with a width of 640m on Ship Shoal would infill with sand within 5 years, that bed load would play the largest role in sediment transport and infilling in sandy borrow areas. These hypotheses remain to be tested, however. By studying sediment character and infilling rates at Caminada Borrow Area, we will test these hypotheses and gain a better understanding of the impacts and future of dredging projects in coastal Louisiana, particularly on Ship Shoal. For example, if the sandy dredge pit deposits are high quality sand from sediment redistribution on Ship Shoal, that means the sand resources are renewable, thus can be used for future coastal restoration projects. Otherwise, if dredge pit sedimentation is mainly muddy, it may influence biologic activity and benthic communities, and reduce Ship Shoal's suitability as a sand resource for future coastal restoration (Stone et al., 2009). This information will inform coastal resource managers and allow for better decision-making ability on future coastal restoration projects.

The objectives of this study were: (1) to quantify seasonal changes in deposition within the sandy Caminada Borrow Area using Beryllium-7 (^{7}Be) as a tracer for short-term sedimentation; (2) to understand process of sedimentation within Caminada Borrow Area, whether by, i) Atchafalaya and/or Mississippi river plume and floods, ii) resuspension and advection of coastal sediments from the outside during events, or iii) wall slope failure; and (3) provide recommendations to future coastal restoration projects about the effects of dredging of inner shelf shoals and the renewability of coastal sand resources.

Figure 1. Location of sand borrow areas on the Louisiana continental shelf, including Ship Shoal (outlined in black line and dotted texture) and Caminada Borrow Area, the focus of this study. Caminada Headland and Elmer's Island received the sand dredged at Caminada Borrow Area. Also shown are paleo-channel "mud-capped" dredge pits (Raccoon Island and Sandy Point; Peveto Channel further west not shown), and the CSI-06 monitoring station. (modified from Xu et al, 2016)

2. Study Area

2.1. Headland, barrier island, and shoal formation in the Mississippi delta

Previous research on the Holocene Mississippi delta established that delta complexes and associated barrier islands and shoals are products of delta-building cycles (Frazier, 1967; Roberts, 1997). The Mississippi delta cycle introduced by Roberts (1997) includes three phases of distinct deposition patterns: briefly, a new delta rapidly forms with increasing discharge due to stream capture by way of a new preferred river course. Over time, the cycle enters a phase of stability where the sediment input and relative sea level rise due to subsidence are in proportional balance. Finally, channel abandonment and relative sea level rise results in deterioration of the delta, and river-derived sands are reworked into erosional headlands, barrier islands and submarine shoals (Penland, 1988; Roberts, 1997). In the delta cycle model, submarine shoals form subaqueously after erosion of headlands and barrier islands due to continued subsidence.

Caminada headland is a product of the Lafourche delta lobe that began prograding ~1,500 years ago (1.5 ka) and deteriorating ~0.6 ka due to an upstream avulsion (Frazier 1967, Törnqvist 1996; Chamberlain et al., 2018). Located ~85 km south of New Orleans and 80 km from the mouth of the modern Mississippi River mouth (see Fig 1), it is comprised of ~22 km of sandy beach ridges backed by and interspersed with finer-grained saltmarsh deposits. Using digital elevation models and volumetric calculations, Miner et al. (2009) quantified the net sediment erosion in the Caminada headland area from 1880s to 2006 as 1.05 (± 0.15) × 10^9 m^3, with a maximum vertical erosion of -10 m. In an effort to combat this retreat, Louisiana Coastal Protection and Restoration Authority (CPRA) spent $137 million for barrier island/restoration as part of the Caminada Headland Beach and Dune Restoration Project (CPRA, 2017); Ship shoal was chosen as the sand resource for this mitigation project, as described below.

2.2. Ship Shoal and Caminada Borrow Area

Ship Shoal is a sandy inner-shelf shoal ~50 km long, 5-12 km wide, at water depths ~8 m, and sand thickness 5-6 m aligned parallel to the shoreline (see Fig 1; Williams et al., 2011). Previous research by Penland et al. (1989) determined Ship Shoal was produced by submergence and marine reworking of a former Mississippi River delta barrier island complex, specifically the Maringouin Delta complex—representing the oldest sand body in the Mississippi delta plain (Frazier, 1967). There exists a greater landward slope indicating that it is migrating due to transgressive deltaic processes, outlined by Penland et al. (1989).

Ship Shoal sediments are categorized into 3 facies, from top to bottom as, shoal crest, shoal front and shoal base, containing a total 1.22 billion m^3 of sand (Penland et al., 1986, Stone et al., 2009, Williams et al., 2011). The upper 4 m of sediments, identified as the shoal crest, are subject to high energy wave and current winnowing and sorting, thus containing very well-sorted, well rounded quartz sand (up to 99 vol%) as well as abundant interclasts of *Crassostrea sp.* (Penland et al., 1986). Shoal front facies are located under and seaward of the shoal crest, containing moderately sorted, fine to very fine-grained sand (75 – 95 vol%) with interclasts of *Crassostrea sp.* (Penland et al., 1986). Sediments of the shoal base consist of interbedded silty clays and wavy bedded poorly sorted, very fine-grained sands (65 – 70 vol%; Penland et al., 1986).

In 2013, the Caminada Headland Restoration Project began as a two-part project and was completed in 2017. In total, 8.7 million cubic yard (6.7 million m^3) of sediments were dredged from Caminada Borrow Area on eastern Ship Shoal and transported 31 mi (50 km) to the aforementioned Caminada Headland, restoring over 4.0 km^2 and 22 km of beach from Port Fourchon to Elmer's Island (Coastal Engineering Consultant Inc., 2017; Fig. 1). Design depth of Caminada Borrow Area is 45 ft (13.7 m) below sea level (Coastal Engineering Consultant Inc.,

2017), or a pit depth of ~5.7 m below eastern Ship Shoal mean elevation. Surface area of the borrow pit totals 495 acres (2.0 km^2; Coastal Engineering Consultant Inc., 2017).

3. Methods

3.1. Field Data Acquisition

Coring field work was conducted on LSU Coastal Studies Institute's R/V Coastal Profiler in August, September, and November 2017, and May 2018 (Table 1). Core locations were identified based on geophysical surveys conducted in August 2017 that revealed the distribution of sandy and muddy material both inside and outside of the borrow area (Liu et al, 2019; see Figure 2). Sampling locations are distributed with 5 locations inside and 2 locations outside of the Caminada Borrow Area (see Fig 2).

Samples were collected using an Ocean Instruments MC400 multicorer and submersible vibracorer. A total of 10 vibracores were collected on August 2 and November 6, 2017 using 5 m-long aluminum core barrels (Fig 2). Previous vibracores have been collected on Ship Shoal by researchers in Louisiana Geological Survey, U.S. Geological Survey (USGS), Coastal Protection and Restoration Authority (CPRA) and Bureau of Ocean Energy Management (BOEM) (Penland et al, 1988; Kindinger et al, 2001; Motti and Kulp, 2003; Khalil et al, 2007), however this study is the first to take place in a sandy dredge pit post-dredging. Vibracores were capped and sealed with electrical tape in the field and returned to the lab for gamma bulk density and p-wave velocity, described below. The cores were then split lengthwise for in-depth lithologic logging, and subsampled at different lithologies for grain size analysis, described below.

A total of 10 multicores at 5 stations were collected on September 17, 2017 and May 8, 2018 using an Ocean Instruments MC400 multicorer (collects 4 cores 10 cm wide, up to 55 cm in length; Fig 2). Although penetrating shallower in depth compared to the vibracorer, this method preserves the sediment-water interface as well as minimizes compaction and destruction of stratigraphy. Two out of the four cores retrieved from each station were chosen for analysis: one was extruded on board into 2 cm-thick subsamples (sealed in Whirl-Paks®) for

radiochemistry and grain size analysis; the other was subsampled using a plastic x-ray tray (dimensions: ~60 cm x 8 cm x 2 cm) and imaged with x-radiography, described below. Both coring methods have been successfully used in mud-capped dredge pits "MCDPs" in Louisiana (see Obelcz et al, 2016; Xu et al., 2016; O'Connor, 2017). Upon return to the lab, all samples were stored in refrigerated conditions in cold rooms prior to sedimentological and stratigraphic analysis.

Table 1. Core information collected during field cruises

Location	Core #	Date Collected	Latitude (degree)	Longitude (degree)	Depth (m)	Length (cm)
			Vibracores			
2	CA17-2A	11/6/2017	28.9142	-90.621	13.19	260
3	CA17-3A	11/6/2017	28.9113	-90.625	13.33	200
3	CA17-3B	11/6/2017	28.9112	-90.625	13.29	200
4	CA17-4A	11/6/2017	28.9161	-90.612	12.78	150
4	CA17-4B	11/6/2017	28.9160	-90.612	12.85	165
5	CA17-5A	8/2/2017	28.9117	-90.611	12.90	250
8	CA17-8A	11/6/2017	28.9165	-90.628	8.46	340
11	CA17-11A	11/6/2017	28.9185	-90.605	8.65	120
Tripod	CA17-TriA	11/6/2017	28.9116	-90.616	13.06	70
Tripod	CA17-TriB	11/6/2017	28.9116	-90.616	12.99	350
			Multicores			
2	CA17-MC2	9/17/2017	28.9140	-90.621	13.30	54
3	CA17-MC3	9/17/2017	28.9113	-90.625	13.23	16
4	CA17-MC4	9/17/2017	28.9160	-90.612	12.94	41
5	CA17-MC5	9/17/2017	28.9116	-90.611	12.86	4
11	CA17-MC11	9/17/2017	28.9184	-90.605	8.89	6
2	CA18-MC2	5/8/2018	28.9143	-90.621	13.20	54
3	CA18-MC3	5/8/2018	28.9113	-90.608	13.53	32
4	CA18-MC4	5/8/2018	28.9162	-90.612	12.93	54
5	CA18-MC5	5/8/2018	28.9116	-90.611	12.92	4
11	CA18-MC11	5/8/2018	28.9184	-90.605	9.05	6

See Figure 2 for core locations.

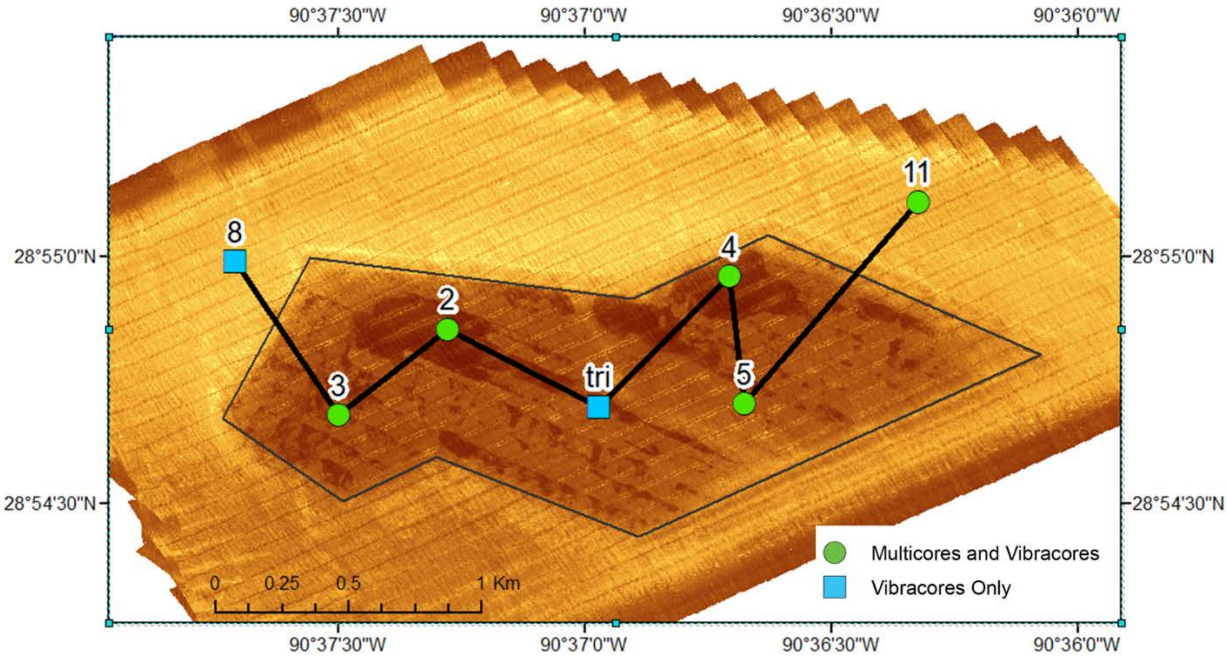

Figure 2. Map of Caminada Borrow Area on Ship Shoal. Coring locations for this study are highlighted in white, and transect line for Figure 3 in black. Background map is from sidescan sonar data collected using EdgeTech 4600 Swath Bathymetry and Side Scan System in August 2017 showing difference in reflection intensity between the muddy (low intensity – dark brown) and sandy (high intensity – light brown) deposits (modified from Liu et al, 2019).

3.2. Multi-Sensor Core Logger and Core Description

A Geotek MSCL-S Multi-Sensor Core Logger was used to measure bulk density of the vibracores in 1 cm intervals. Bulk density is quantified using a ^{137}Cs gamma source that emits a beam of gamma rays which is attenuated by the core and measured by a detector located on the opposite side. The amount of attenuation is calculated based on this emission and detection (Geotek Ltd., 2018). Calibration is done empirically by measuring an aluminum cylinder with various diameters that represent known sediment porosities, sealed with water inside an aluminum liner (from 0-50% porosity). Gamma bulk density logs provide important information about changes in lithology and porosity: in materials with high density, the emitted gamma ray is absorbed and scattered more, resulting in a high gamma attenuation value; conversely, in materials with low density or high porosity, the emitted gamma ray passes through more easily,

resulting in a lower gamma attenuation value. These logs, in addition to manual lithologic descriptions of split cores, are used to correlate detailed stratigraphy across the borrow area.

3.3. Grain Size Analysis

Multicore and vibracore subsamples were analyzed for grain size using a Beckmann-Coulter laser diffraction particle size analyzer (LDPSA) with an Aqueous Liquid Module (ALM) that has a measurement range 0.017 µm to 2000 µm. Samples are prepared by mixing ~2 g of wet sample with 2 ml of 30% hydrogen peroxide in a test tube and left to digest overnight to remove organic matter. As the reactions finished, 15 ml of sodium metaphosphate (25 g/L) is mixed in and allowed to sit overnight to deflocculate the sample. Each sample was vortex mixed, sieved for large particles using an 850-micrometer sieve, and sonicated prior to measurement. Grain size data from LDPSA for each core is then aggregated using Sigmaplot® to generate frequency contour plots, which highlight grain size distribution changes down core.

3.4. X-Radiography

At each multicore station, one core was preserved in plastic trays for x-ray imaging to evaluate fine details of stratigraphy and any bioturbation. Trays were imaged using a Thales Flashscan 35 digital X-ray detector illuminated by a Medison Acoma portable X-ray. Digital images were taken in greyscale RAW format and converted to JPEG using ImageJ image software, adjusting for brightness, contrast and clarity. Images were digitally stitched due to the size limitations of the detector plate. Light shades represent higher density and larger grain sizes (coarse silt/fine sand), while darker colors represent lower density and finer grain sizes (fine silts/clays). Brightness/intensity profiles down core were plotted using ImageJ to quantify the interlayered stratigraphy between fine and coarse silts.

3.5. Radiochemistry Analysis—calculation of short-term sedimentation

For this study, short-term sedimentation rates were measured using the radioisotope ^{7}Be, which has a half-life of 53.2 days. Beryllium-7 forms in the atmosphere due to cosmogenic reactions (Baskaran et al, 1993). The constant fallout of this radionuclide signifies ^{7}Be is a good tracer for short term sediment accumulation (Baskaran et al, 1993, Kaske and Baskaran, 2011, Keller et al., 2016, Restreppo et al., 2019).

Multicore subsamples are prepared by dehydrating in a laboratory oven set at 55ºC immediately upon arriving back in the laboratory and taking mass measurements before and after to calculate water content. Dried samples are then homogenized with a mortar and pestle and packed into petri dishes. Care is taken to analyze ^{7}Be samples within one half-life ($t_{1/2}$=53.2 days). Samples are counted on Canberra REGe and BEGe germanium detectors calibrated for energy and efficiencies for 24 hours following methods of Cochran and Masqué (2003), and Keller et al (2016) for a spectrum of energy levels. Activity of ^{7}Be is associated with a peak at 477.6 keV.

Inventory of ^{7}Be for each core (dpm cm^{-2}) can be calculated using Eq. 3 from Muhammad et al. (2008):

$$I = \Sigma \rho_s \Delta z (1 - \phi_i) A_i \qquad (1)$$

where ρ_s is grain density (g/cm^3, assumed to be 2.65 g/cm^3), Δz is thickness of subsample (2 cm), ϕ_i is porosity calculated from water content loss at 55°C (%), and A_i is activity at depth (dpm g^{-1}). To determine if sediment focusing occurs at out study area, theoretical ^{7}Be inventories were identified (Courtois, 2018). Annual dry and wet deposition flux of ^{7}Be was found to be 5.4 dpm cm^{-2} from Barataria Bay, LA (Corbett et al, 2004) to 14.7 dpm cm^{-2} y^{-1} at Galveston, TX (Baskaran et al, 1993).

With SigmaPlot software, we are able to calculate sedimentation rates by exponential decay regression analysis using method from Muhammad et al. (2008):

$$A_z = A_0 \mathrm{e}^{\left(-\lambda z / S\right)} \qquad (2)$$

where A_z is activity at depth z (dpm g^{-1}), A_0 is activity extrapolated to the surface (dpm g^{-1}), λ is the decay constant (4.76/year for ^{7}Be) and S is sediment deposition rate (cm/day).

4. Results

4.1. Sedimentary Environment of Caminada Borrow Area

Fig. 3a shows a schematic lithologic cross section of the sandy borrow area from vibracores collected, plotted over a bathymetric transect taken in 2018 (bathymetry provided by Haoran Liu; transect location shown in Fig. 2). The depth inside the borrow area is around 13 m and 5 m outside. Outside of the borrow area (Cores 8 & 11) we find clean undisturbed well sorted fine sand beds with abundant interclasts of *Crassostrea sp.*, representative of ambient Ship Shoal material similar to shoal crest and shoal front sequences described by Penland et al. (1986). The gamma-derived bulk density of this material outside of the Caminada borrow area measures ~2.0-2.1 g/cm^3 and the grain size is 2.5 – 3.5 ϕ (100 – 200 μm) (Fig 3b; see also Appendix A, B). Core stratigraphy inside the pit (Cores 2, 3, 4, and Tri) generally shows 5 – 25 cm of mud deposited on top of fine sand beds (40 - 70 cm thick; Figs 3a & b). One location (Core 5), however, had fine sand at the surface and interclasts of *Crassostrea sp*. All of these cores inside the pit had older, muddy deposits at depth (> 85 cm depth; Figs 3a & b). Bulk density logs show that surface sediments (<10 cm depth, muddy) typically displayed relatively low values (1.5-1.8 g/cm^3, see Fig. 3b for an example; Appendix A & B shows the results for all cores). Below this, the gamma bulk density of the sand bed at 10-70 cm depth is ~2.1 g/cm^2 with a grain size of 2.5 – 3.5 ϕ (100 – 200 μm; Appendix A, B), consistent with Ship Shoal sand measured from outside of the borrow area (Fig 3b). Bulk density subsequently decreases to ~1.85 g/cm^2 and grain size to 4.5 – 6 ϕ (16 – 48 μm) below these sand horizons (70-170 cm; Fig 3b; Appendix A, B).

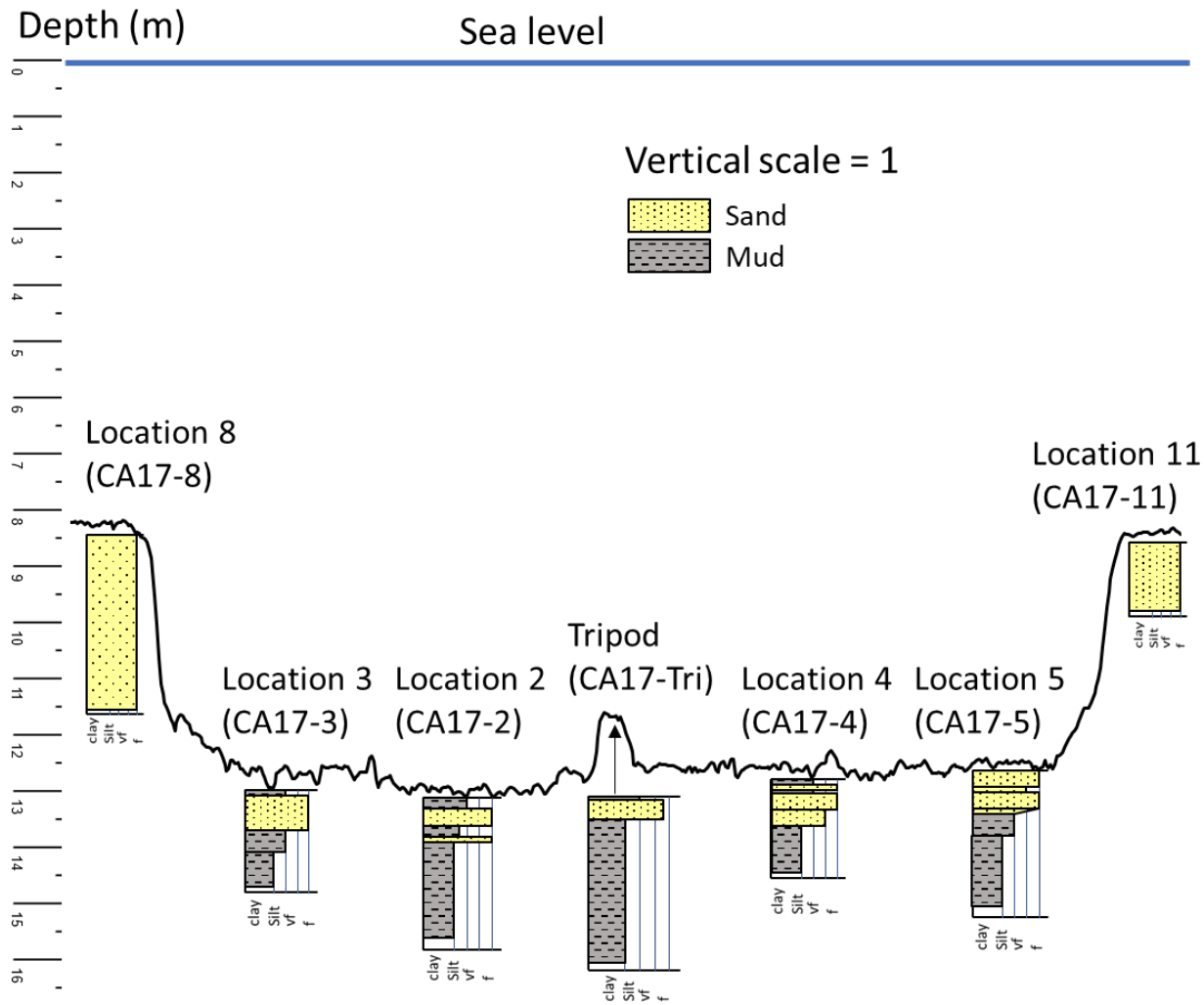

Figure 3a. Cross section of Caminada Borrow Area combining detailed sedimentary descriptions of split vibracores to scale. Cores show 5 – 25 cm of mud deposited inside the borrow area on top of sandy beds, interpreted as lower Ship Shoal sand deposits; below which we find mud sequences, interpreted as older deltaic deposits. On the outside of the borrow area, we find clean undisturbed sand beds representative of shoal crest and shoal front (Penland et al, 1986). See Fig. 2 for core and transect locations.

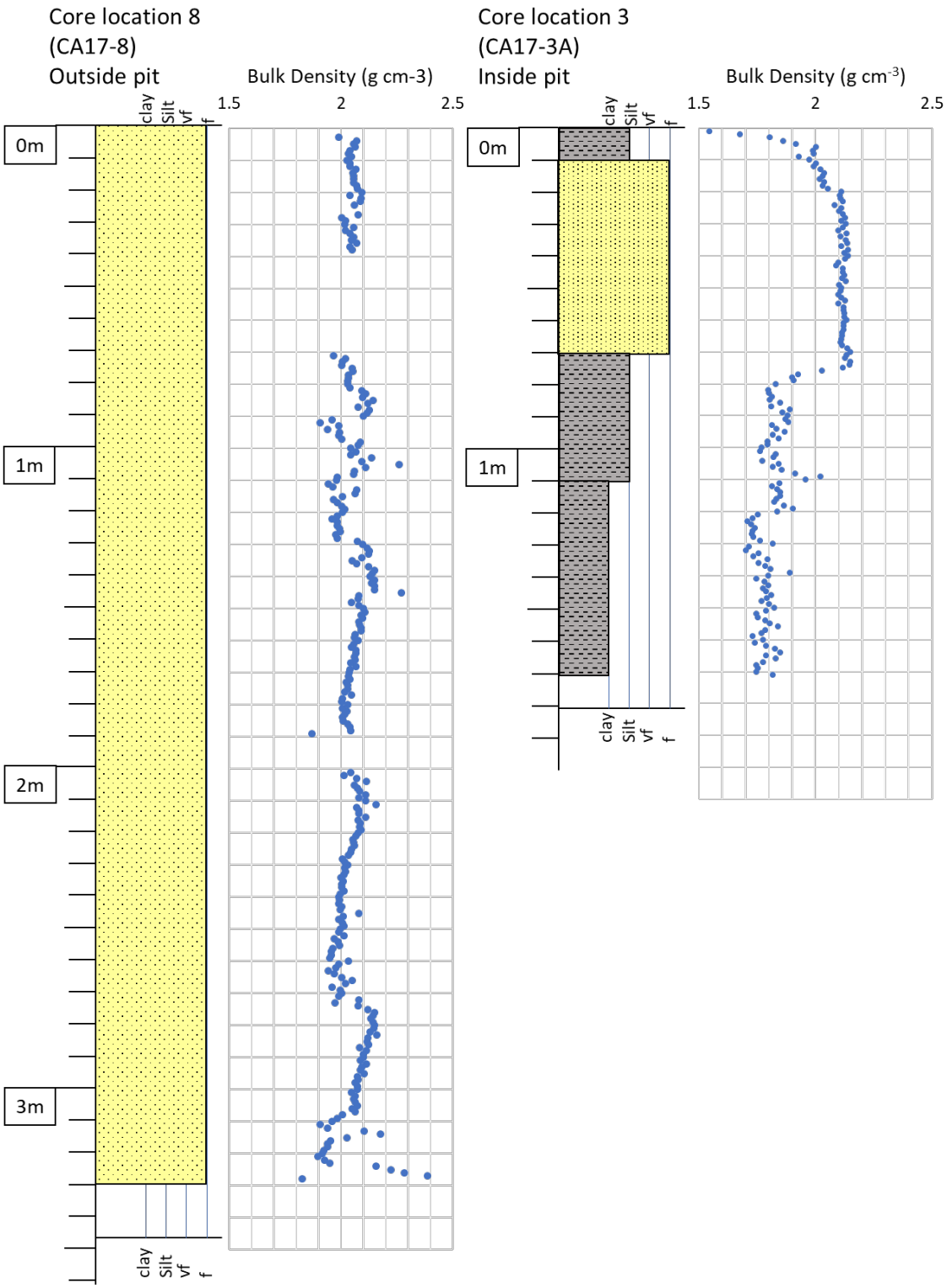

Figure 3b. Core description and gamma density log for a typical core located outside of the pit (CA17-8, left see Fig. 2 and Table 1 for location) shows all fine sand. In comparison, core description and gamma density log for a typical core located inside the pit (CA17-3A, right) shows clear lithological changes from 10 cm of surficial mud, to 60 cm of very-fine/ fine sand, followed by silt/clay at depth. I

4.2. Multicore Grain Size and X-rays

Grain size analysis of multicore sediments indicate that the material in-filling Caminada Borrow Area is dominated by silts at 50 – 80% by volume (Fig 4). On average, multicore grain sizes have a mode around medium to coarse silt, ranging from at 4.5 – 6 ϕ (16 – 48 μm; Fig. 4). Only occasionally are very fine to fine sand laminations measured (averaging 2.5 – 3.5 ϕ, 100 – 200 μm; Fig. 4).

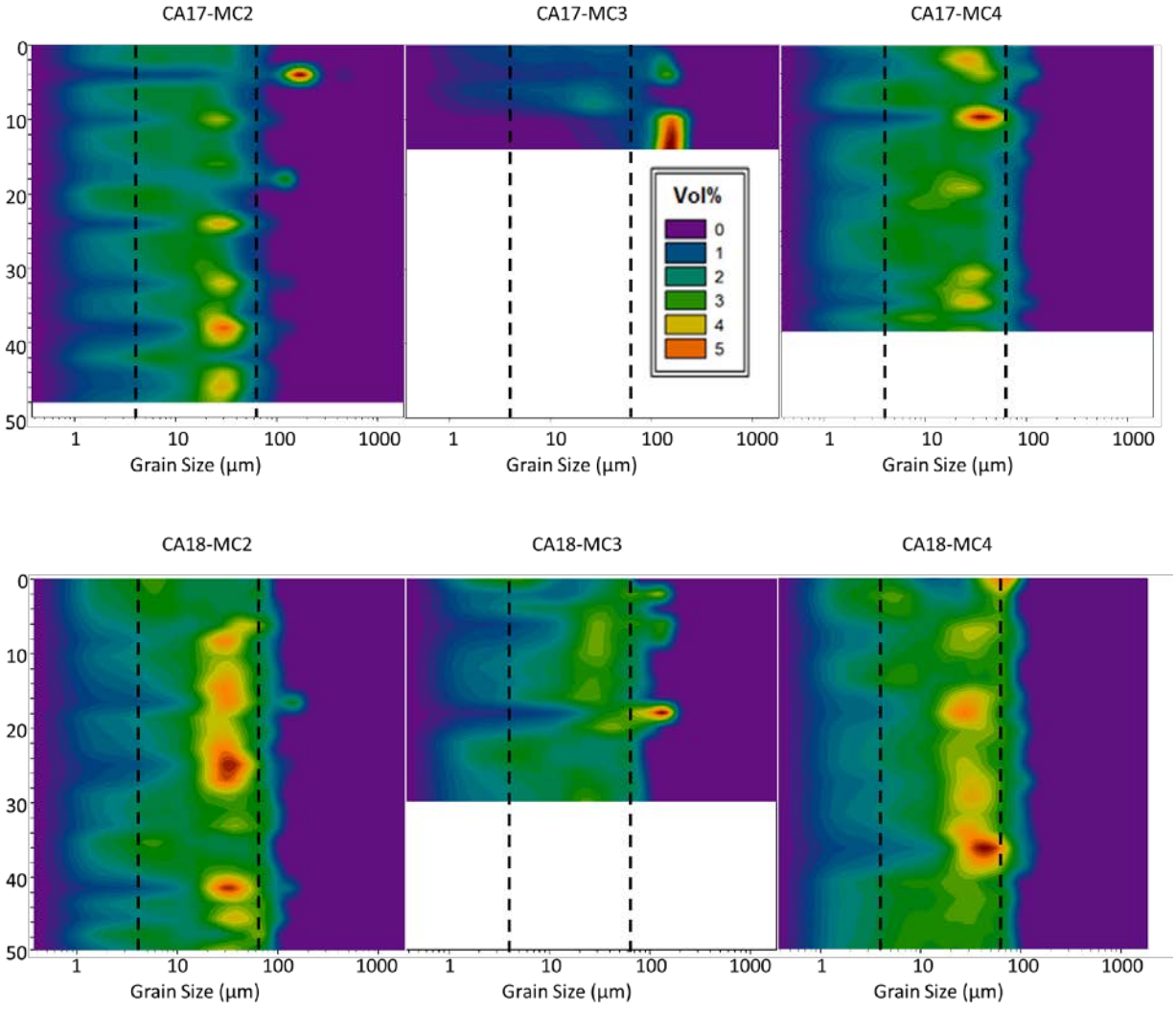

Figure 4. Filled-contour plots of grain size for multicore samples inside Caminada Borrow Area in 2017 (top) and 2018 (bottom) with warmer colors corresponding to higher frequencies. Vertical dashed lines indicate division between clay, silt and sand size sediments. Grain sizes are predominantly medium-coarse silt with a few laminations of very fine to fine sand.

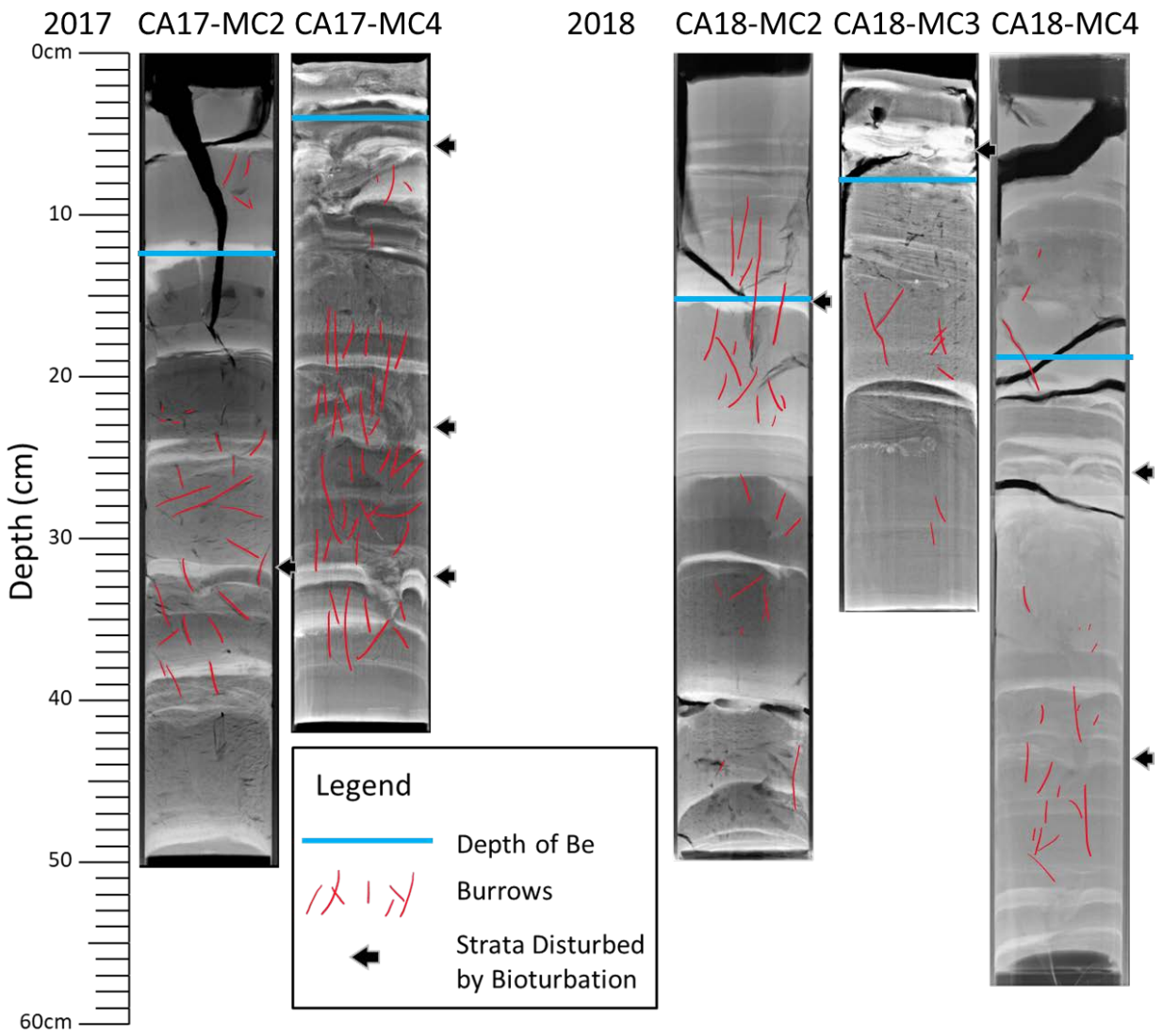

Figure 5. Annotated x-ray images of multicores taken in September 2017 and May 2018. Light colors represent higher density and larger grain sizes (coarse silt/v. fine sand), while darker colors represent lower density and finer grain sizes (fine silts/clays). Blue lines for each core represent depth of ^{7}Be penetration. Red lines are annotated burrows. Black arrows are sediments disturbed by bioturbation commonly found in the region (Bouma, 1968). Black in the x-ray image represents cracks formed by dewatering prior to x-ray analysis. See appendix E for original images.

Similarly, x-radiographs show packages of clays and fine silts separated by planar laminations of coarser silt 10 – 15 cm apart, as confirmed by particle size analysis described above (see Figs. 4 & 5). Specifically, in both 2017 and 2018, MC-2 and MC-4 showed 5-10 cm of dark, finer grained sediments separated by coarser lighter grained sediments, possibly periodic

higher energy sedimentation or individual event beds. Burrows can be seen in all cores as dark grey linear features not oriented to bedding. Sections also display disruption of bedding due to possible bioturbation (see 2017 MC-4 at 5 cm and 32 cm, Fig 5).

4.3. Radiochemistry Analysis

Cores collected in October 2017 showed Beryllium-7 was present at depth for three of the five cores collected, these three extracted from the muddy sediment in Caminada Borrow Area (Locations 2, 3, and 4; Fig 2). The maximum depth of ^{7}Be penetration in 2017 ranges from 4 cm to 12 cm, averaging 8 cm (Fig 6). Peak ^{7}Be activity is observed at top-most samples and ranges from 3.92 +/- 0.54 dpm g^{-1} to 9.14 +/- 0.70 dpm g^{-1}. In 2017, ^{7}Be activity trend shows a correlating exponential decrease with depth in these three cores. Calculated ^{7}Be inventory ranged 0.62 to 3.67 dpm cm^{-2} and sedimentation rates from 0.02 to 0.07 cm d^{-1}, averaging ~0.05 cm d^{-1} (see Figs. 6 & 7; Table 2). Inventories of ^{7}Be are less than equilibrium inventories expected for wet and dry precipitation for the region of 5.4 - 14.7 dpm cm^{-2} (Baskaran et al., 1993; Corbett et al 2004). Two Multicores did not show beryllium in their samples: CA17-MC5 and CA17-MC11. Both cores were taken where surface sediment was sand rich—confirmed by grain size analysis—from within a sandy area inside Caminada Borrow Area and outside, respectively.

In the repeat coring campaign executed in May 2018, sites were reoccupied to obtain comparable seasonal sedimentation rates (see Table 2). Cores were similarly found to have muddy and sandy surface sediment composition (Fig. 4). Beryllium-7 was present to depths for the same three muddy locations within Caminada Borrow Area (Locations 2, 3, and 4; see Figs 2 & 6). Maximum depth of ^{7}Be penetration was much deeper than in October 2017, ranging from 8 cm to 16 cm, averaging 12.6 cm (Fig 6). Peak ^{7}Be activity ranges from 5.76 +/- 0.78 dpm g^{-1} to 9.18 +/- 1.01dpm g^{-1}. CA18-MC2 shows ^{7}Be trend of exponential decrease with depth, with an inventory of 2.60 to 2.85 dpm cm^{-2} and sedimentation rate of 0.15 cm/d (Fig 6; Table 2). Similar

to 2017, inventories of ^{7}Be are less than equilibrium inventories expected for wet and dry precipitation for the region of 5.4 - 14.7 dpm cm^{-2} (Baskaran et al., 1993; Corbett et al 2004). CA18-MC4 display intermittent peaks and irregular downward trend in ^{7}Be, preventing the determination of an accurate sedimentation rates in the core (Fig. 6). Instead, minimum sedimentation rate is calculated by dividing depth of penetration with 4 half-lives, yielding 0.08 cm/d. The cores collected in the sandy environments inside and outside the pit (CA18-MC5 and CA18-MC11, respectively) did not contain any detectable ^{7}Be.

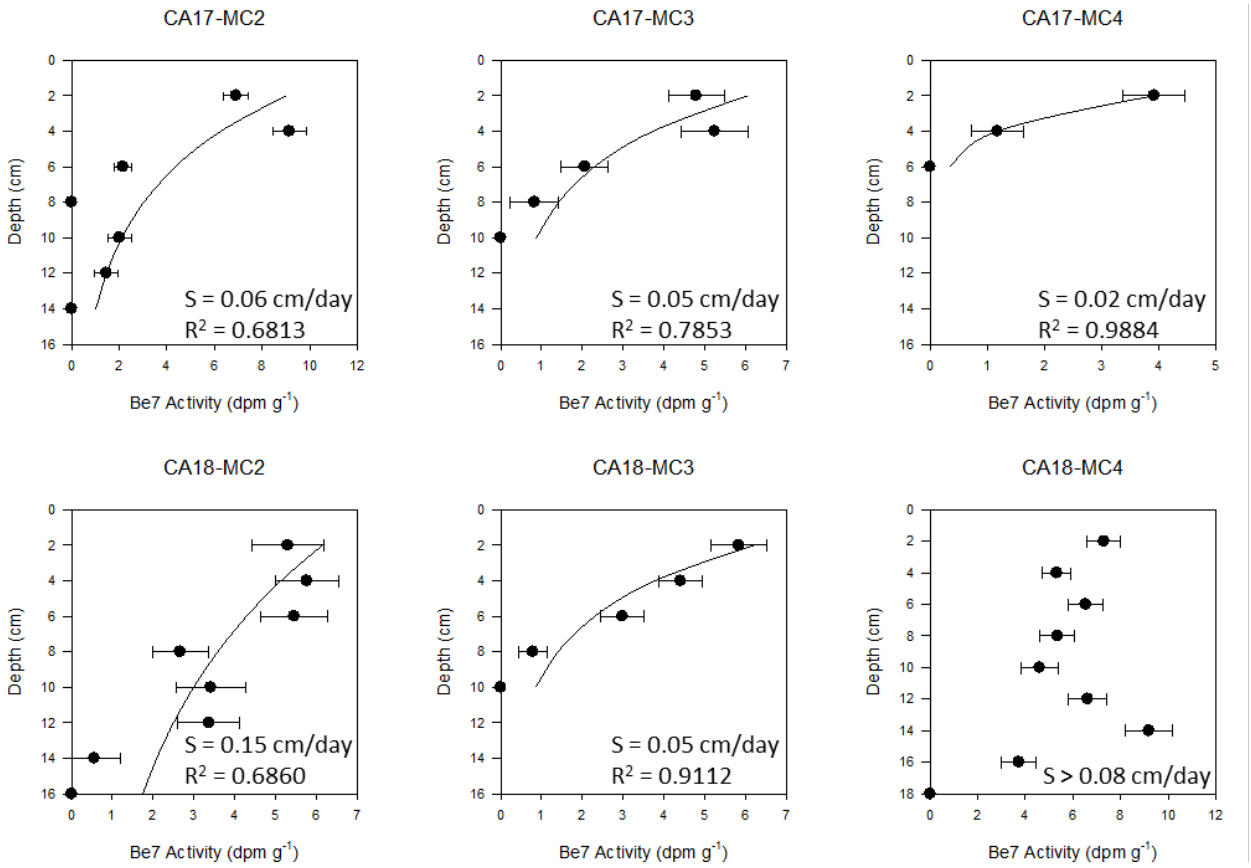

Figure 6. Beryllium activity at depth from Caminada Borrow Area at locations 2, 3 and 4 (locations shown in Fig. 2). Depth of ^{7}Be penetration increased from 6-14 cm in Fall 2017 to 8-16 cm in Spring 2018. Deposition rates increased from 0.02-0.07 cm/day in Fall 2017 to 0.05-0.15cm/d in Spring 2018. For CA18-MC4, minimum deposition rate is calculated due to the irregularity of ^{7}Be activity.

Table 2. ^{7}Be depth of penetration, inventory, and calculated sedimentation rates in Oct 2017 and May 2018

			Depth of Be^{7} Penetration (cm)		Be^{7} Inventory (dpm cm^{-2})		Sedimentation Rate (cm day^{-1})	
Location	lat	long	2017	2018	2017	2018	2017	2018
2	28.9142	-90.6213	12	14	3.673	2.614	0.059	0.145
3	28.9113	-90.6250	8	8	2.125	2.603	0.057	0.052
4	28.9160	-90.6118	4	16	0.613	2.854	0.019	>0.08

See Fig 2 for core locations.

5. Discussion

5.1. Sandy Borrow Area Sedimentation

Lithologic description of vibracores from within Caminada Borrow Area showed dredging operations left 30-80 cm of sandy material with grain sizes consistent with cores taken on the outside of the pit (2.5 – 3.5 Φ or 100 – 200 μm; Fig 3b). We interpret these sandy beds to be representative of transgressive Ship Shoal sand facies (i.e. shoal front, described as very fine sand with grain size 2.7 – 3.3 Φ by Penland et al, 1986), which overlay older regressive deltaic mud sequences, also presented by Penland et al. (1986). We interpret the 5-25 cm thick mud layers at the surface of the vibracores as recently infilled material post-dredging, evidenced by multicore grain size and x-ray results, and laden with ^{7}Be allowing the calculation of recent sedimentation rates (Fig 6). Figure 7 plots multicore grain size, x-ray image, image brightness curve, and beryllium activity profile results together to illustrate the distinct coarse silt laminations within fine silts and clays. This fine grained sediment could be sourced from many locations, as sedimentation along Ship Shoal, like the entire Louisiana continental shelf, is influenced by Atchafalaya and Mississippi surface and benthic plumes (Wells and Kemp 1981, Stone et al., 2004, Wright et al., 2001, Allison et al., 2012, Denommee et al., 2016), wind-driven currents (Murray 1998, Walker and Hammack 2000, Stone et al., 2009), and storm waves (Bentley et al., 2002, Kobashi et al., 2007).

Specifically, sediment infilling the Caminada Borrow Area could include: i) slope failure/adjustment, and redistribution of Ship Shoal sands, which would contribute to sandy deposits; ii) Mississippi and Atchafalaya river plumes during high and low discharge season, fluid mud deposition, and storm-related resuspension of silts and clays, which would contribute to fine grained sediment deposits. If sedimentation within the borrow area is sandy, meaning infilling sediments originates mainly from slope adjustment and redistribution of Ship Shoal

sands, then the renewable sandy borrow area may be used for future restoration projects in Louisiana. Otherwise, if sedimentation within the borrow area is clay and silt rich, meaning sedimentation originates from hypopycnal river plumes, benthic suspensions of fine-grained sediments, and resuspension of fine sediments from inner shelf or bays (Wright et al., 2001, Rotondo et al 2003), then the change in ocean-bottom substrate from sandy to muddy may have biologic activity and benthic communities and reduce the suitability for future use. Our results suggest the sediment infilling the pit is predominantly a combination of material sourced from river plumes and resuspension along the shelf, and pit wall failure appears to be insignificant, as discussed in detail below.

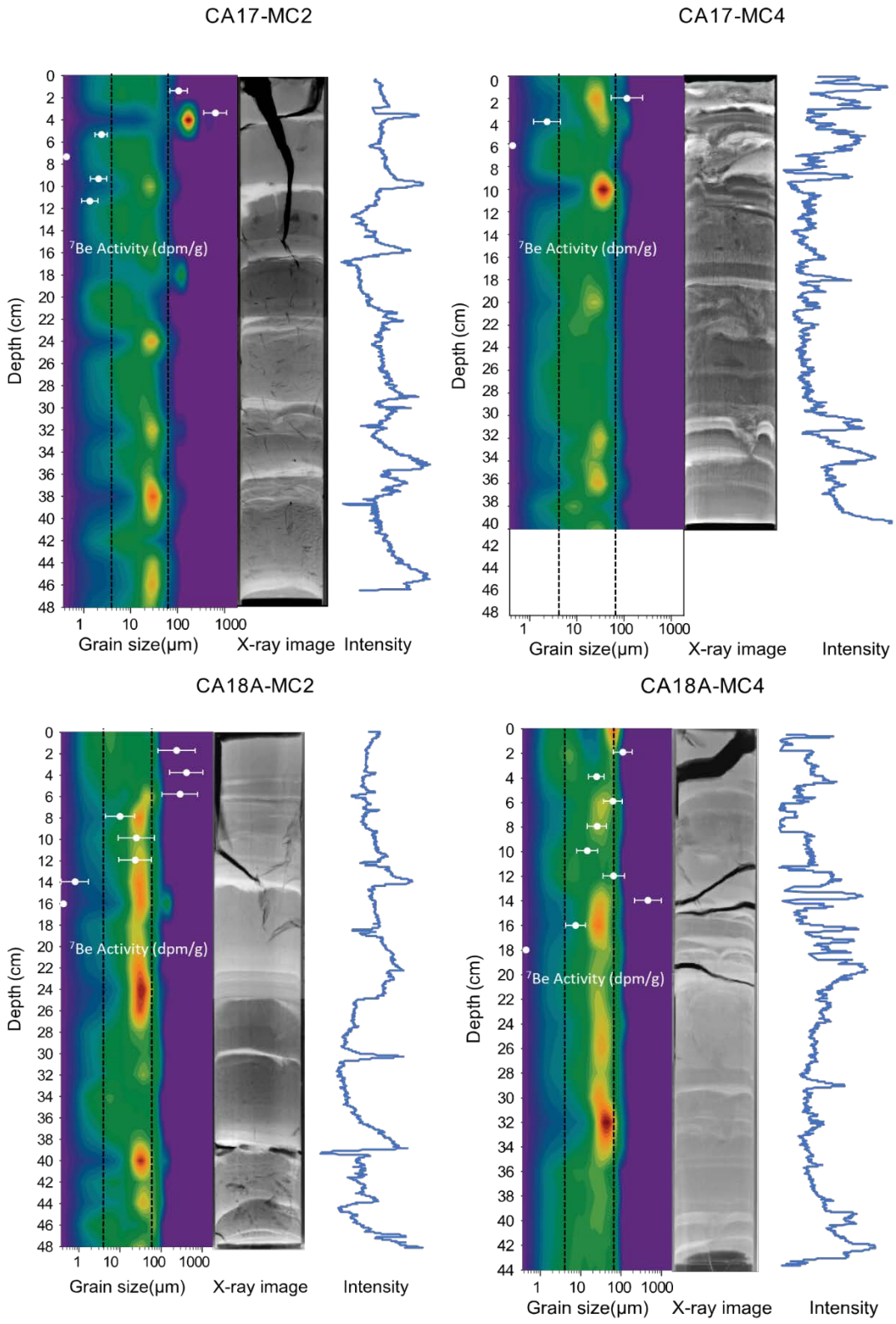

Figure 7. Plots of multicore grain size, beryllium activity, x-ray imagery, and down-core brightness, illustrating bright, variably spaced, silty laminations

5.1.1. Pit Wall Failure or Sediment Readjustment

Pit wall failure and sediment redistribution on Ship Shoal would reintroduce sandy sediments into Caminada Borrow Area from the wall slope and beyond. These processes would deposit Ship Shoal sand with grain sizes of 2.5 – 3.5 Φ (100 – 200 μm, this study; Penland et al, 1986) into the borrow area. In this study, the vast majority of coarse sediments found in multicores (-MC2, -MC3, -MC4) within the borrow area have grain sizes in the coarse silt range 4.5 Φ (48 μm; Fig. 5) with the only exception at coring location 5, where the substrate is sandy at the top as observed in both vibracores and multicores (Figs 2, 3, Appendix B). Thus, the grain size difference in the coarse-grained infilling sediments of Caminada Borrow Area and original Ship Shoal sand means that the repeating coarse silt laminations within the multicores is not a result of wall slope failures post-dredging operations, but perhaps episodic higher-energy events such as storm passage. In addition, Liu et al. (2009) confirmed through bathymetry and backscatter sonar measurements that infilling sediment type is more muddy than sandy, where only ~3% of infilling material between year 2017-2018 had been wall adjustment confined to the margins of the borrow area. This is contradictory to Nairn et al.'s (2005) model that reported bed load playing the largest role in sediment transport and infilling in sandy borrow areas.

5.1.2. Recent ^{7}Be-laden Sediment Deposition from River Plumes

Beryllium – 7 (half-life ~ 53 days) is predominantly produced from spallation of oxygen and nitrogen in the atmosphere to material eroded from terrestrial origins and transported by rivers into the marine environment (Sommerfield et al., 1999). Detected ^{7}Be activity found in Caminada Borrow Area thus indicates recent sedimentation from a fluvial input, in this case sourced from the Atchafalaya or Mississippi Rivers. Figure 8 shows the seasonal and spatial variability of recent sediment deposits in Caminada Borrow Area from beryllium penetration depth, inventory and sedimentation rate (data from Table 2). As mentioned previously, ^{7}Be depth

increased from Fall 2017 to Spring 2018 (from 8 to 13 cm, on average), resulting in ^{7}Be inventories that increased from 2.14 to 2.69 dpm cm^{-2}, respectively (Fig 8). Seasonal sedimentation rates yielded by ^{7}Be in the Fall 2017 to Spring 2018 revealed an increase in sedimentation from 0.02-0.06 cm/day to 0.05-0.15 cm/d. This increase in sedimentation reflects the seasonal floods of the Mississippi and Atchafalaya river plumes (e.g., Baskaran et al., 1993; Restreppo et al, 2018). Allison et al (2012) determined a six-fold increase in daily sediment transport during seasonal peak flood discharge of Mississippi and Atchafalaya Rivers. This indicates the highest amount of river plume-derived sedimentation and ^{7}Be inventory should occur soon after peak flood. Inventories of our coring sites (0.61 – 3.7 dpm cm^{-2}) are comparable to studies along the Louisiana coast such as the Chenier Plain (maximum 1.2 – 5.4 dpm cm^{-2}; Rotondo and Bentley, 2003). In comparison, O'Connor (2017) has much greater ^{7}Be inventories, which we estimate to be over 10 dpm cm^{-2} at both Sandy Point and Racoon Island (based on calculations with ^{7}Be activity and depth of penetration assuming similar porosity and grain density). Inventories of ^{7}Be in Caminada Borrow Area are lower than theoretical steady state atmospheric inventories 5.4 – 14.7 dpm cm^{-2} found by Baskaran et al (1993) and Corbett et al (2004). This result is consistent with Corbett et al (2004) results on the Mississippi River delta front where measured inventories were below steady state inventory from the atmosphere fallout in the Spring. Corbett et al (2009) suggests that this was likely due to the large ratio of drainage basin to deposition areas such as in the case of the Eel River (Sommerfield et al, 1999) and Mississippi River (Corbett et al, 2004; Courtois 2018). The lower ^{7}Be inventories is consistent with the irregularities of ^{7}Be profile down cores (Fig. 6), which suggests mixing of different sources with different residence times (as seen by O'Connor, 2017).

Further comparisons with previous dredge pit studies on the Louisiana continental shelf show other sites have received greater sedimentation and ^{7}Be penetration depths, and this appears to be related to proximity to river source as well as variable seasonal discharge. O'Connor (2017) determined sediment accumulation rates from cores taken in two muddy, paleo channel dredge pits Sandy Point and Raccoon Island in July 2015 (location in Fig. 1). Sandy Point dredge pit is located proximal to the Mississippi River (12.5 km northwest of Grand Pass, 25 km northwest of Southwest Pass); Raccoon Island dredge pit is farther from the Mississippi River, but closer to the Atchafalaya River (147 km west of Southwest Pass, 65 km southeast of the Atchafalaya River). For comparison, Caminada Borrow Area in this study is more distal from either river source: 117 km to the west of Southwest Pass and 90 km to the southeast of the Atchafalaya River. Average accumulation rates at Sandy Point and Raccoon Island were 0.145 cm/d and 0.24 cm/d, respectively, in July 2015 (O'Connor, 2017), which is greater than the 0.05 cm/d for Caminada Borrow Area in September 2017 and 0.10 cm/d in May 2018 (this study), thus proximity to river source appears to have some control on sedimentation rates observed. We also note that sediment accumulation is related to variable seasonal discharge: the average discharge reported for the Mississippi River by O'Connor (2017) for the 6 months prior to core extraction was ~40,000 $m^3 s^{-1}$, noticeably greater than what occurred in the six months prior to our core extraction 2017 and 2018 (11,000 and 31,000 $m^3 s^{-1}$, respectively; described further below).

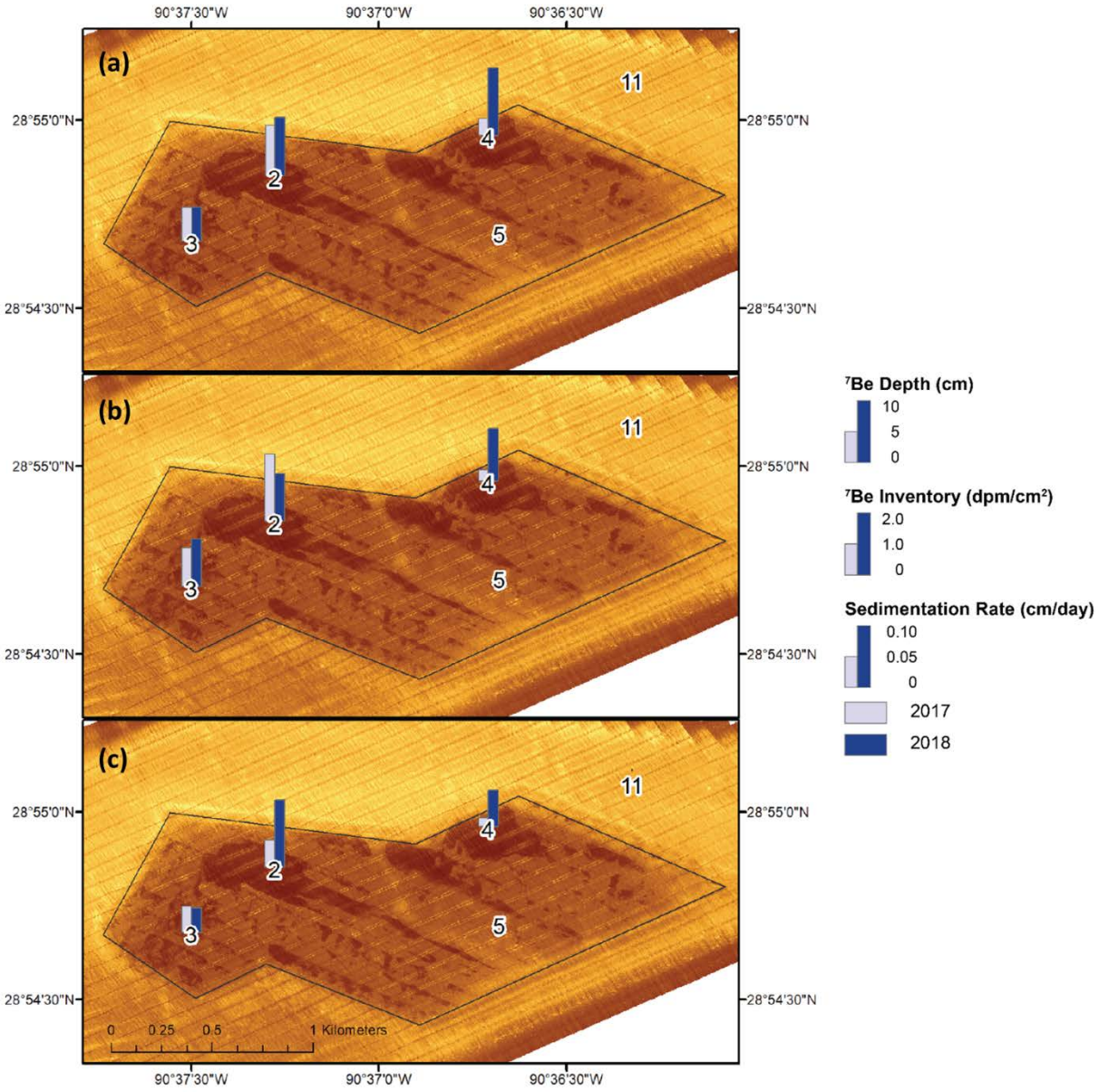

Figure 8. Beryllium penetration depths (a), inventory (b) and sedimentation rate (c) plotted in ArcGIS over sidescan sonar map generated in 2018 by Liu et al (2019) showing seasonal and spatial variations. Darker browns show muddy, low reflectivity sediments and lighter browns show sandy sediments. Note coring location 2 and 4 are located on muddy substrate and location 3 is on majority muddy substrate. See table 2 for listed information

Discharge data from US Army Corp of Engineers was used to further evaluate the relationship between river discharge and sedimentation rates in Caminada Borrow Area: daily river discharge data were downloaded from River Gages website (rivergages.com) at Atchafalaya River at Simmesport and Mississippi River at Tarbert Landing stations from the

periods 6 months (~200 days, or 4 half-lives due to ^{7}Be detection limits) prior to coring dates. Increase in average sediment accumulation rates in Caminada Borrow Area from 0.05 cm/d in 2017 to 0.10 cm/d in 2018, along with increased average beryllium penetration depths from 8 cm to 13 cm correspond with an increase in discharge between the two periods. Average discharge in the 6 months leading up to coring dates increased from 18,931 $m^3 s^{-1}$ to 20,358 $m^3 s^{-1}$ for the Mississippi River and 8,197 $m^3 s^{-1}$ to 8,921 $m^3 s^{-1}$ for the Atchafalaya River (Fig 9). The timing of peak river discharge varied between 2017 and 2018 (2017: 5/23/2019, 3.5 months prior to coring; 2018: 3/16/2019, 2 months prior to coring). This also appears to correspond with greater sedimentation rates (0.05 cm/d in 2017, 0.10 cm/d in 2018; Fig 8). It is interesting to note in the 2 months leading up to coring dates, river discharge is much higher in 2018 than it was in 2017 Mississippi/Atchafalaya: 11,000/5,000 $m^3 s^{-1}$ in 2017 compared to 31,000/14,000 $m^3 s^{-1}$ in 2018; Fig 9). Again, this was less than documented for the Mississippi River in 2015 (O'Connor, 2017).

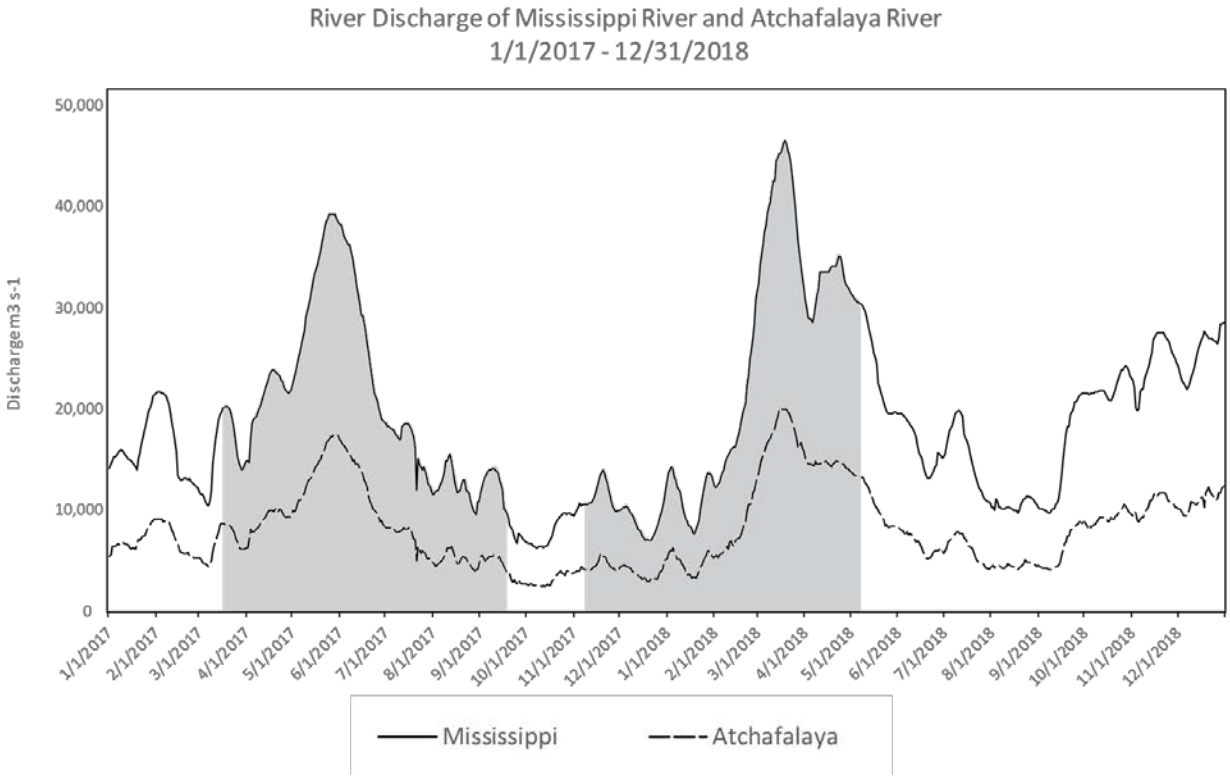

Figure 9. Discharge of Atchafalaya (dashed line) and Mississippi (solid line) Rivers in 2018 plotted as $m^3 s^{-1}$. Daily discharge data from US Army Corps of Engineers website, RiverGages.com; Shaded time periods are six months leading up to core retrieval.

To further determine if fluvial sediment in Caminada Borrow Area is derived from the Mississippi River or the Atchafalaya River, we analyzed geo-referenced MODIS (Moderate-Resolution Imaging Spectroradiometer) satellite imagery of hypopycnal plumes provided by Louisiana State University's Earth Scan Laboratory. Using GIS, Mississippi and Atchafalaya surface river plumes polygons were mapped from 65 clear-sky coastal satellite images for the six months leading up to our coring dates (Figure 10b, c). In 2017, the Caminada Borrow Area appears to be impacted by both the Atchafalaya river plume as well as the Mississippi river plume (Fig 10b). However, in 2018, only the Atchafalaya river plume extends to the Caminada Borrow Area on Ship Shoal, while the Mississippi River plume only rarely extends to Ship Shoal (Fig 10c). This result is consistent with shelf sediment dispersal models predicting a sediment "mixing area" near Ship Shoal where both the Atchafalaya and Mississippi River influence local

sedimentation (Xu et al, 2011). This result of Atchafalaya hypopycnal surface plume extending over Ship Shoal is also consistent with those observed by Walker and Hammack (2000), Kobashi et al. (2007) and Stone et al. (2009). However, Zang et al. (2019) found in a two-decadal sediment dynamics model for the northern Gulf of Mexico region, a limited impact of fluvial sediments affecting sedimentation on sandy shoals. Instead, sediment dynamics was modeled to be mainly affected by strong wind events between October and April (Zang et al., 2019). The discrepancy in river plume coverage may be a result of atmospheric wind patterns or events, or due to benthic resuspensions not detectable through satellite imagery.

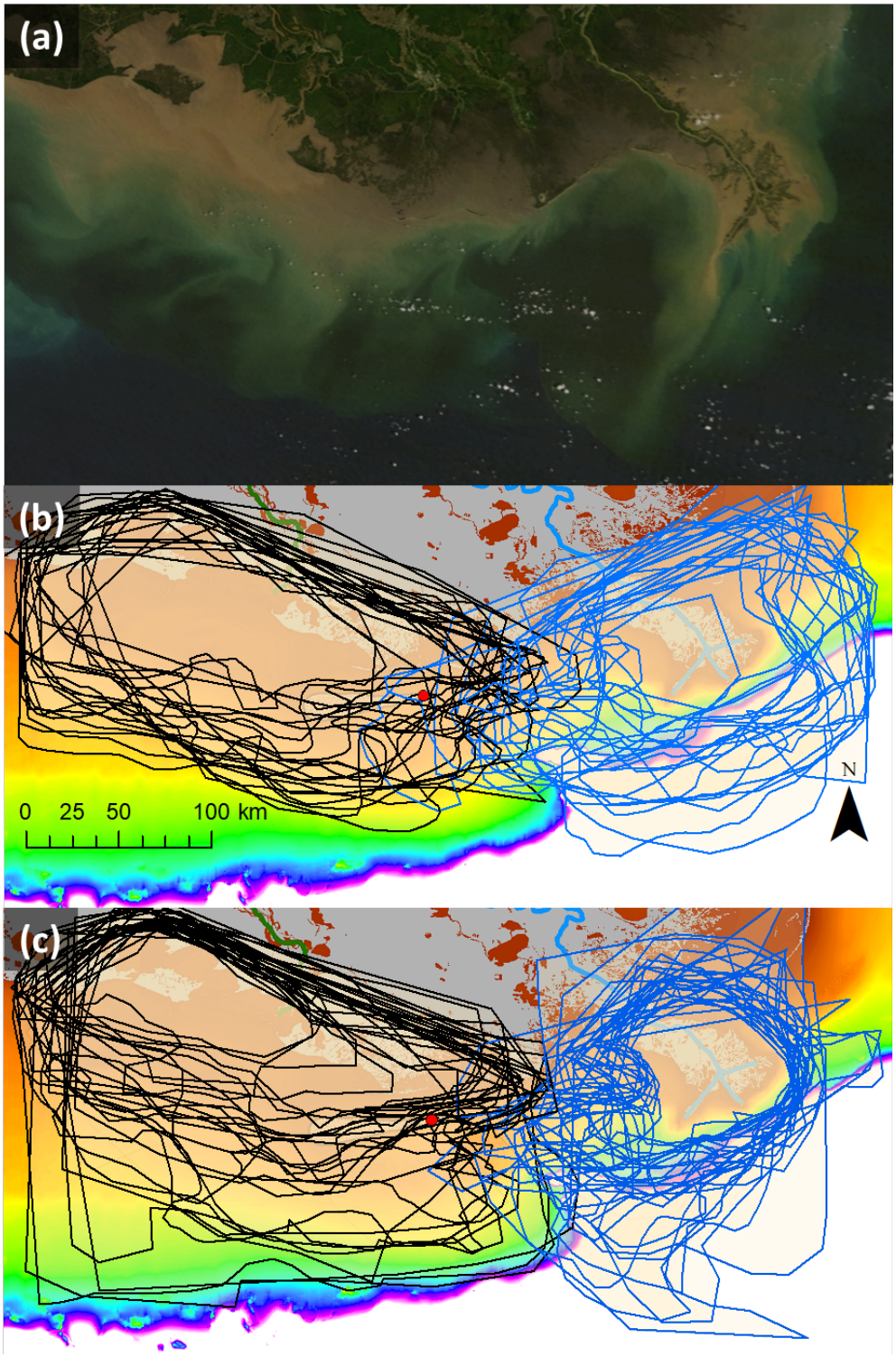

Figure 10 a, b and c. a, Earthscan lab image from 04/15/2018 showing regions of high sediment concentration, either from hypopycnal river plumes or sediment resuspension on the shelf; b and c, Stacked polygons of Mississippi (Blue) and Atchafalaya (Black) river plumes mapped from 65 MODIS true color images for the 6 months period leading up to the coring dates (b: 3/17/2017-9/17-2017, c: 11/8/2017-5/8/2018). Red circle is the study site, Caminada Borrow Area. MODIS satellite Imagery provided by LSU Earth Scan Laboratory.

5.1.3. Atmospheric and Oceanographic Effects of Storm Events on River Plumes and Sediment Deposition

Interestingly, O'Connor (2017) similarly found a lack of ^{7}Be activity surrounding borrow areas. At Raccoon Island, it was hypothesized that the dredge pit was capturing benthic resuspended sediments, and preventing further resuspension due to the lower wave base within the pit (O'Connor, 2017). Raccoon Island's exceptionally high sediment accumulation rate despite its distance from fluvial sediment source can be attributed to capturing abundant fluid mud transport originating from the Atchafalaya river and oceanographic conditions allowing for frequent resuspensions of sediments (Rotondo and Bentley 2003, Kobashi et al., 2007, O'Connor 2017). This means, in addition to the correlation between higher measured sedimentation rates and the proximity to a river source, oceanographic and atmospheric conditions are more important in some locations (e.g., Raccoon Island; O'Connor 2017; this study).

As discussed, river plume shape and extent are impacted not only by discharge and sediment load, but also by water column dynamics, wind speed and wind direction (Mossa and Roberts, 1990; Moeller et al, 1993; Walker and Hammack, 2000; Cobb et al., 2008). In coastal Louisiana, river sediments are predominantly transported westward due to prevailing winds and currents for most of the year (Wells and Kemp 1981). However, winter or tropical storms can shift river plume shape to extend further west or east (over Ship Shoal, for instance), which can significantly affect sediment transport along the shelf (Walker and Hammack 2000; Kobashi et al. 2007; Stone et al., 2009). Winter storms are low pressure systems that travel from the arctic polar region and pass the northern Gulf coast every 3 – 10 days between October and May (DiMego et al., 1976). During frontal passage, high energic conditions can resuspend coarser sediments such as coarse silts and sands during reworking by storm waves, resulting in erosion and coarse sediment deposition (Corbett et al, 2004; Kobashi et al., 2007; O'Connor, 2017). As

these winter storms or cold fronts pass, wind patterns shift from blowing from the southeast to blowing from the north with a decrease in barometric pressure (Stone et al, 2009). This post-frontal, north-originating wind could cause the Atchafalaya River Plume to transport further southeast, as well as resuspending recently deposited sediments and distributing fine silts and clays on the continental shelf (and Ship Shoal, of particular interest here; Walker and Hammack 2000, Kobashi et al., 2007).

To further understand wind effects on fine sedimentation deposited within Caminada Borrow Area, atmospheric and oceanographic conditions were collected from Louisiana State University's Wave-Current-surge Information Systems (WAVCIS) CSI-06 meteorological and hydrodynamic monitoring station, which provided sustained winds speeds and atmospheric pressure during the six months leading to both coring dates (location shown in Fig. 1). Wind speed and direction data measured hourly are plotted as polar scatter plots and rose diagrams in Fig. 11. The variable wind speeds and directions recorded in the six months prior to coring are consistent with the findings that the plume geometry varies greatly (Fig 10). For example, wind directions during the spring and summer months leading up to the September 2017 coring date (Fig. 11 a, b) show prevailing wind direction from the W with higher-speed winds originating from the N, NE. The N and NE originating winds caused the Mississippi River plume to extend further west, covering the Caminada Borrow Area. In in the winter and spring months leading up to the May 2018 coring date, predominant winds were from the SE and SW, with faster winds originated from the direction NE. Plume geometry responded accordingly (Fig 10b, c).

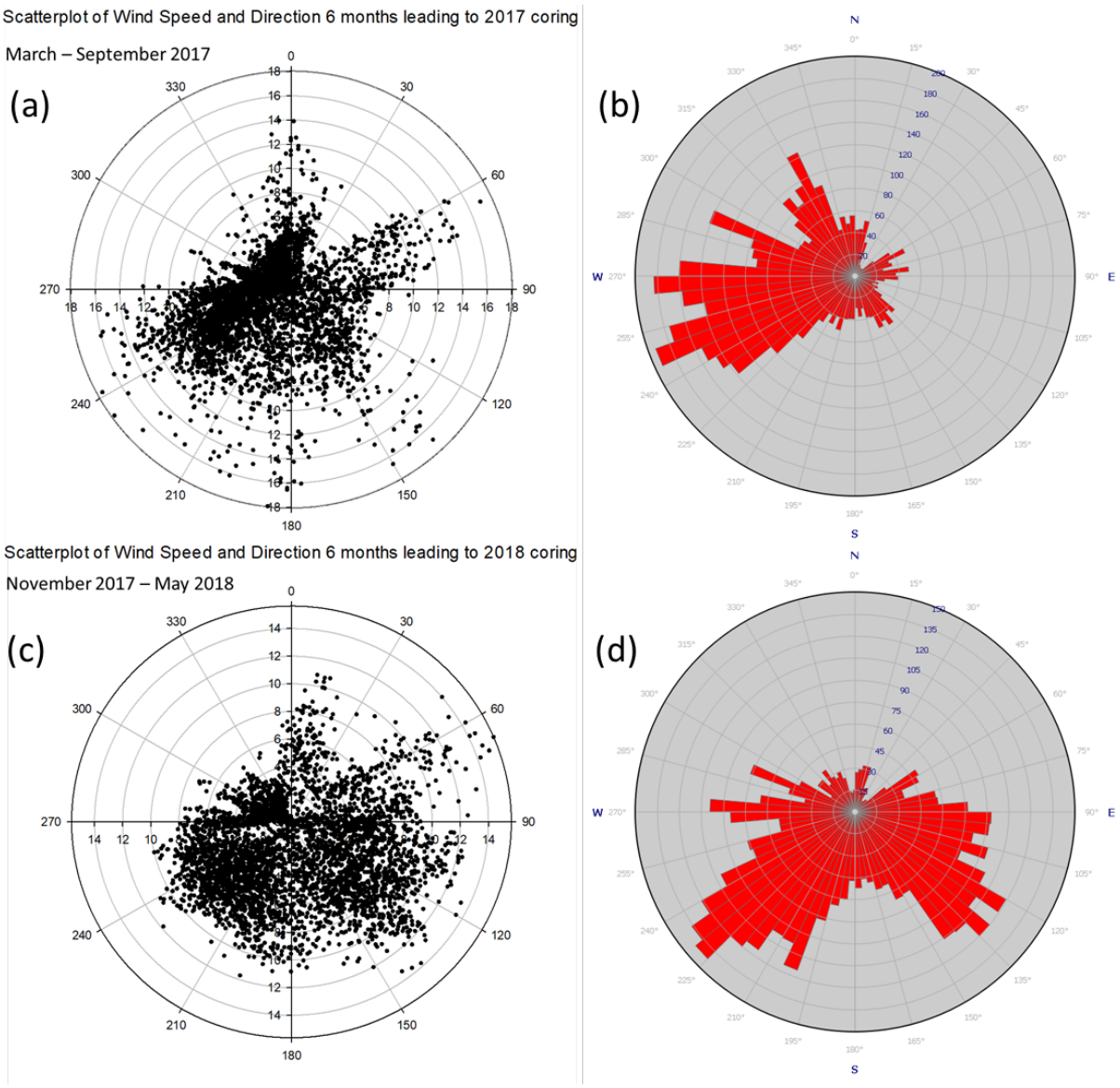

Figure 11. (a) Scatter plot and (b) rose diagram of wind directions in summer 2017 in the six months leading up to coring date (9/17/2017). Note during these months the predominant wind direction is from the West. (c) Scatter plot and (d) rose diagram of 2018 wind directions in the winter and spring months leading up to May coring date (5/8/2018) with predominant wind direction from the SE to SW direction.

Previous work has shown tropical storms including hurricanes can have similar effects on sediment mixing and coarse sediment deposition during passage and post-frontal plume extension that deposits fine sediments (Stone et al, 2009). In addition, much higher (10-1000x) suspended sediment concentrations have been measured near the bed (Allison et al., 2000, Bentley, 2002). In seasons with low discharge and sediment load, hurricanes and tropical storms

can still cause local resuspension, causing sediment cover to shift over Ship Shoal and Caminada Borrow Area (Fig. 10, Stone et al., 2009). To support this, there is a lack of steady-state and high river discharge sedimentation—what O'Connor (2017) described as "Type 1" sediments—at Caminada Borrow Area. Instead, the fine-grained sediments found in Caminada Borrow Area more closely resemble sediments deposited immediately following frontal passages, described as "Type 3" by O'Connor (2017).

To investigate this, LSU's CSI06 daily average wind speeds were plotted with a minimum 10 m/s cutoff next to atmospheric pressure to illustrate high wind events inferred to be cold fronts or tropical storms (Fig 12, Perez et al, 2000; Restreppo et al, 2018). Age-converted multicores showing bright colored, coarse laminations are plotted with this data (Figs 7, 12). Two prominent peaks in wind speed in 2017 corresponds to two hurricanes/tropical storms: on June 22, tropical storm Cindy, and around August 30, hurricane Harvey reached coastal Louisiana, causing spikes in wind speed up to 18 m/s and drops in atmospheric pressure (Fig 12). These high energy wind events were strong enough to resuspend coarse silts and sands on the shelf and redeposit them producing variable event layers that have been seen elsewhere across the Louisiana Shelf (Goni et al, 2007; Walker and Hammack, 2000; Bentley et al, 2000, 2002; Xu et al, 2015). We show here the timing of the 2017 wind events correlates well with the occurrence of coarser grain size (coarse silt) inside the borrow area, suggesting these coarser laminations are related to storm induced deposition (Fig 12). Tropical storm Cindy and hurricane Harvey induced sediment pattern can be seen in satellite imagery covering eastern Ship Shoal and Caminada Borrow Area (Appendix D).

In contrast, 2018 Louisiana had a mild tropical storm season with no major storms. This is confirmed by the wind speed having no strong peaks during that time period (Fig 12). As a

result, sedimentation during Spring 2018 had much less large event layers corresponding with hurricanes or large storms (Fig 12). However, the six months leading up to coring (11/8/2017-5/8/2018) coincides with the winter storm season (October – May, Dimego et al, 1976). The smaller coarse silt laminations are likely formed during these smaller winter storm events, but the correlation does not appear to be strong (Fig 12). One explanation for the less correlatable silty layers in 2018 compared to wind events could be the preservability relating to thickness of these beds as described by Bentley et al (2000 and 2002). The thickness of event beds associated with major hurricanes is greater than those of smaller cold fronts and storms, thus in 2018, the thinner coarse silt laminations may not have been preserved in the borrow area.

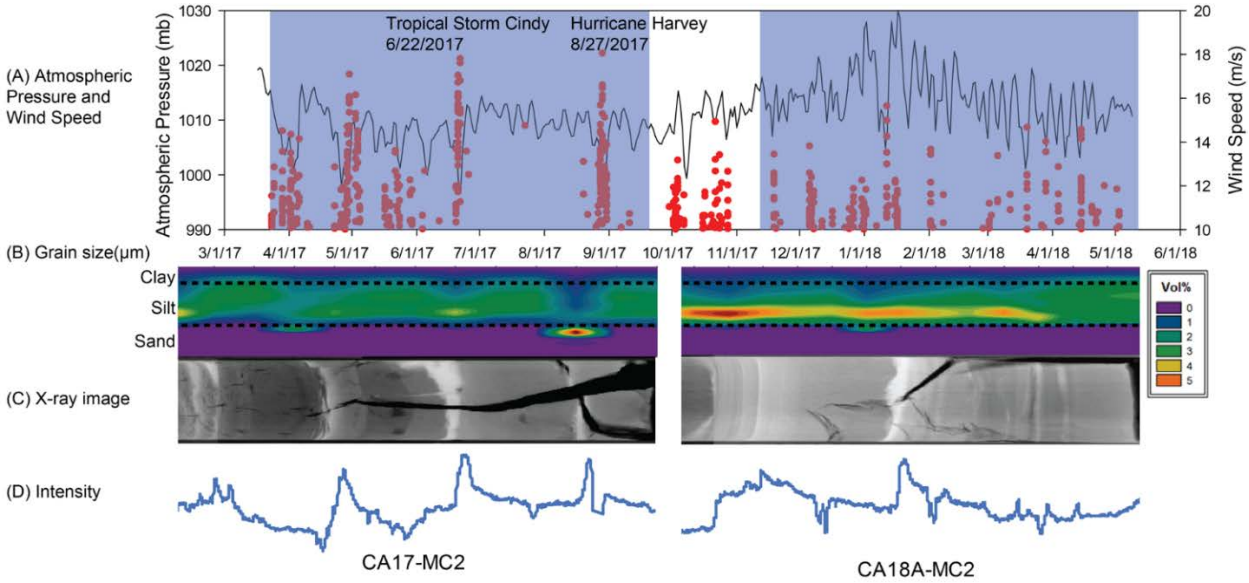

Figure 12. Atmospheric pressure with wind speed (A) with columns of high wind representing a strong wind event, corresponding with a decrease in atmospheric pressure. These events appear to correlate with bright, course silty deposits seen in grain size (B), x-ray image (C), and x-ray image intensity/brightness curve (D) well in 2017 (left), and less so in 2018 (right).

Beryllium – 7 activity derived ages of the coarse silt/sand laminations seen in Fig 12 (brightest in x-ray imagery) are plotted on scatter plots against observed high energy event dates for 2017 and 2018 (Fig 13). In both cases, the calculated ages of the coarse silt/sand laminations correspond to distinct high wind storm events. In 2017, there is a general overestimation of ages

compared to observed events, despite a similar slope. This suggests that while the estimation of sedimentation rate is reasonable (10-15 cm/day), there may have been little sediments deposited after Hurricane Harvey in late August, close to the coring date. In 2018, the calculated ages and observed dates agree in the months of March – April, but diverge further back in January – February.

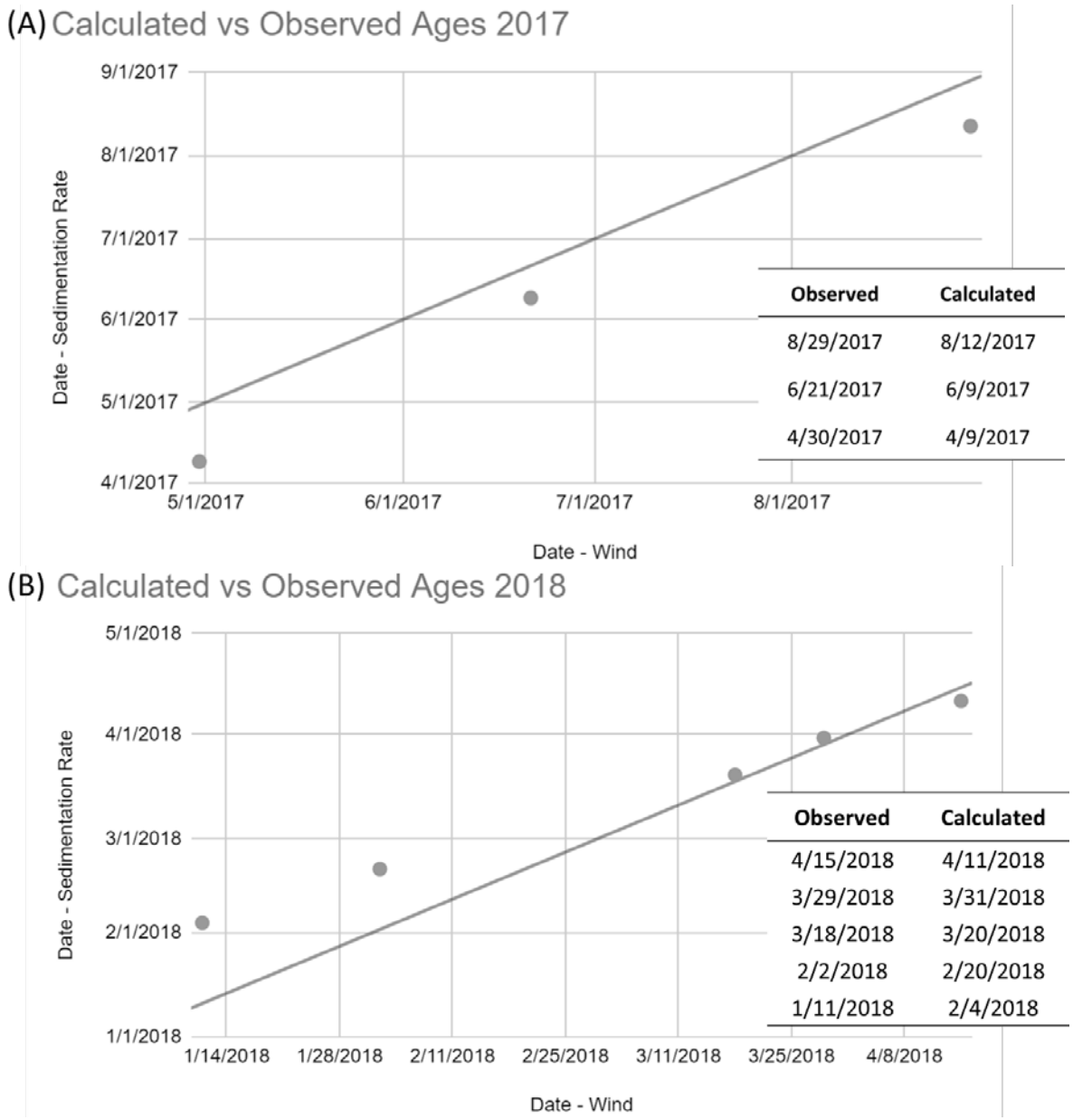

Figure 13. Scatter plots of coarse silt lamination age calculated from sedimentation rates against high wind energy events observed from CSI-06 in 2017 (a) and 2018 (b) (a: 3/17/2017-9/17-2017, b: 11/8/2017-5/8/2018). Grey line shows a slope of 1.

5.2. Implications for Coastal Management of Sand Resources and Borrow Areas

Sediment infilling Caminada Borrow Area is not ambient Ship Shoal sand (as hypothesized by Nairn, 2005), as there is an evident lack of sand within the infilled material inside the borrow area (Figs 3, 5). Core results from this study suggest mainly fine to coarse silts are deposited during post-frontal southeastern movement of the Atchafalaya plume, punctuated by coarser silt deposits during high energy storm events. Furthermore, Caminada Borrow Area is infilling at a slower rate (~ 5 times) than numerical modeling predicted (Nairn et al., 2005, Liu et al, 2019), or exhibited by paleo channel borrow areas more proximal to the Atchafalaya and Mississippi River mouths (Sandy Point and Raccoon Island ~90% more: average sedimentation rates 0.145 - 0.24cm/d, O'Connor, 2017; vs. Caminada: 0.05 - 0.10 cm/d, this study). Nairn et al (2005) suggested sandy dredge pits would exhibit an increased sedimentation rate compared to paleo channels with mud overburden due to bedload transport of sand outside the pit and subsequent deposition inside the pit. From 2017 to 2018, we see an increase in area covered by fine sediments overlaying the original Ship Shoal sands (Liu et al, 2019). Based on the presence of sediments containing ^{7}Be and grain size analysis of the cores taken within Caminada Borrow Area, we determined the sedimentation within Caminada Borrow Area is predominantly river-derived, consisting of mostly fine to coarse silts.

This data suggest new infilling models are needed for future coastal restoration work, particularly for sandy dredge pit environments. Furthermore, due to the dredge pit infilling with finer-grained sediments, sandy shoal restoration-quality sand resources are not renewable in this location. In addition, as a significant amount of new silt and clay are deposited within Caminada Borrow Area, more research into the biochemical impacts of a muddy depression within Ship Shoal is needed to characterize the dredging impacts on benthic communities and water quality.

6. Conclusion

1. In 2017, 4-12 cm of sediments were deposited within a 5-6 month time period in low lying areas in Caminada Borrow Area. Sedimentation rates are calculated to be 0.02 – 0.06 cm/day. During repeat coring in 2018, 8-16 cm of sediments were deposited and sedimentation rates calculated to be 0.05 – 0.15 cm/day. There is little difference in median grain size of 4.5 – 6 ϕ (16 – 48 μm) between the two years. Average ^{7}Be inventory remained similar though spatial variations in 2017 was greater.

2. Clays and fine silts deposited intermittently in the borrow area are likely sourced from the Atchafalaya River plume with some contribution from the Mississippi River plume and resuspension from shelf and bays, as seen from plume geometry recorded by satellite imagery and delineated in ArcGIS. Atchafalaya plume sediments extend southeastward to reach Caminada Borrow Area immediately following winter storms or tropical storms. Resuspension and redeposition during these higher energy winter storm or tropic storm events likely produced coarse silt laminations. Sedimentation in the borrow area is not significantly affected by wall slope failure as seen from the lack of original Ship Shoal sand material in recent core deposits.

3. Sedimentation rates and sediment types are different than predicted by Nairn et al (2005). Infilling rate is slower than predicted (~ 5 times) and the material is mainly silts and clays. More research is needed to understand the impacts of changing to a fine sediment environment. Restoration quality sand on sandy shoals in this location of Louisiana is thus not renewable.

Appendix A. Bulk density

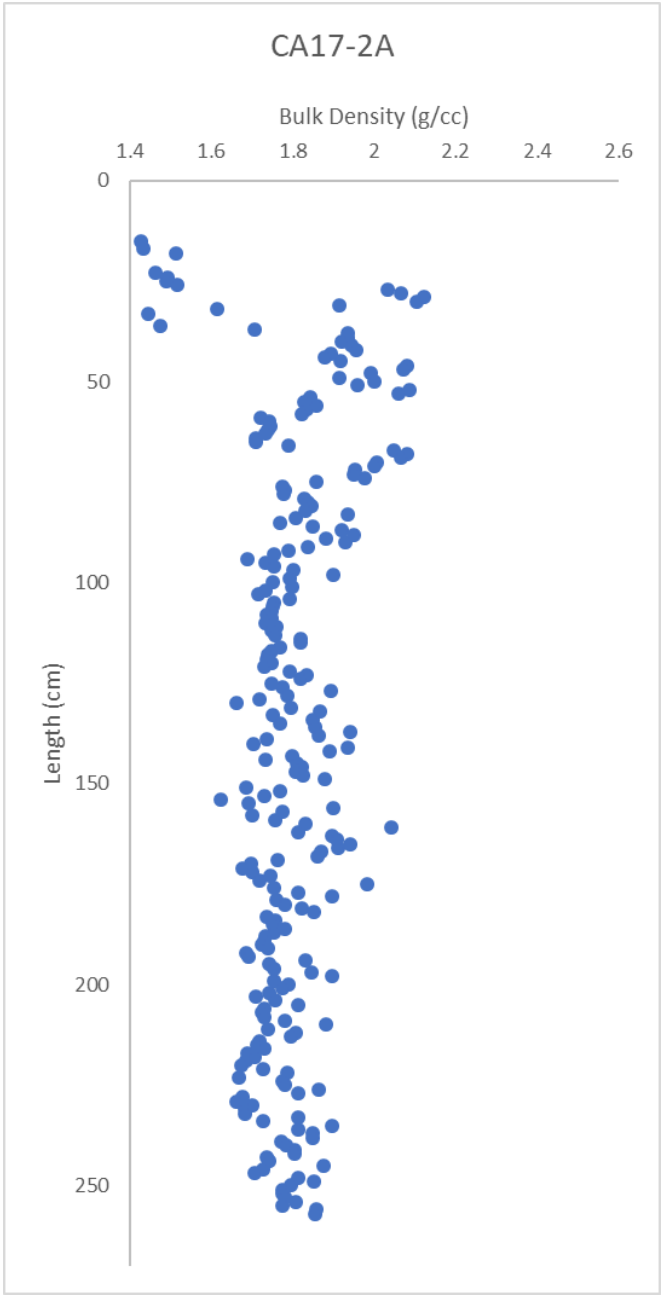

Figure A.1. Gamma derived bulk density plot for vibracore CA17-2A

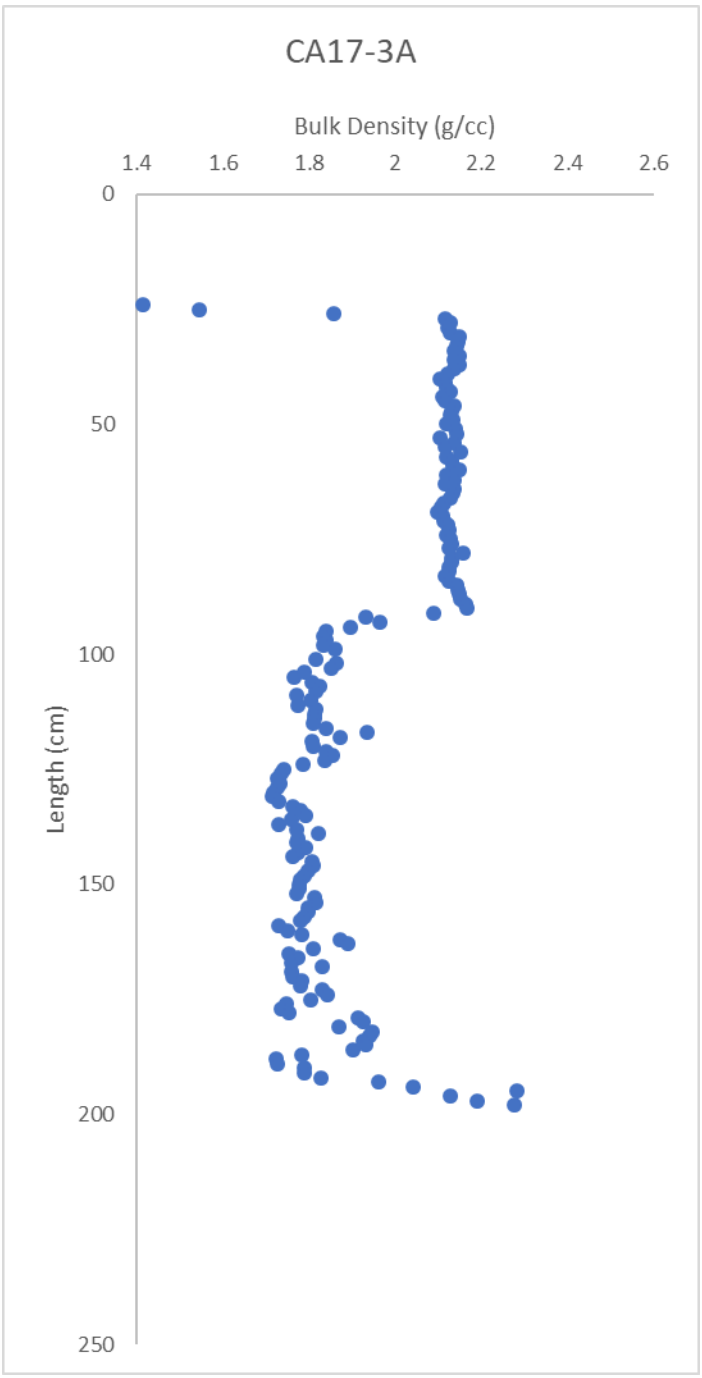

Figure A.2. Gamma derived bulk density plot for vibracore CA17-3A

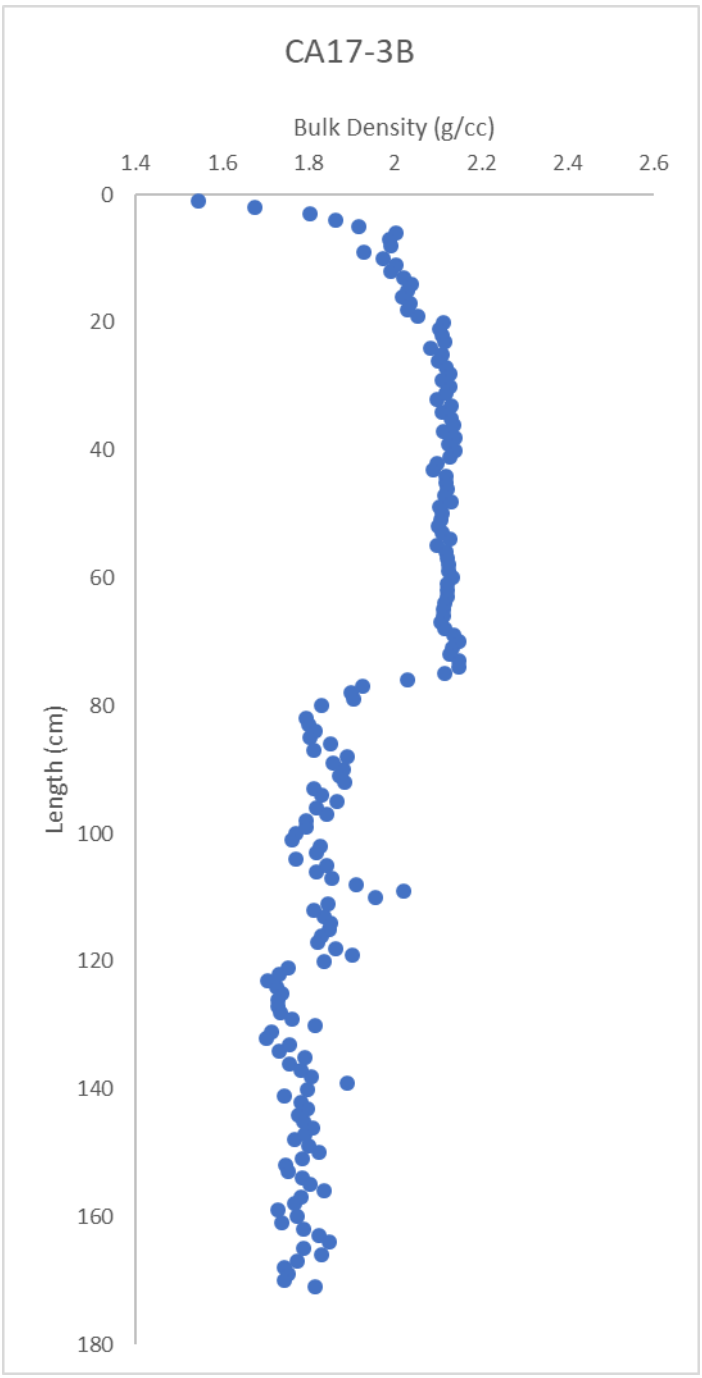

Figure A.3. Gamma derived bulk density plot for vibracore CA17-3B

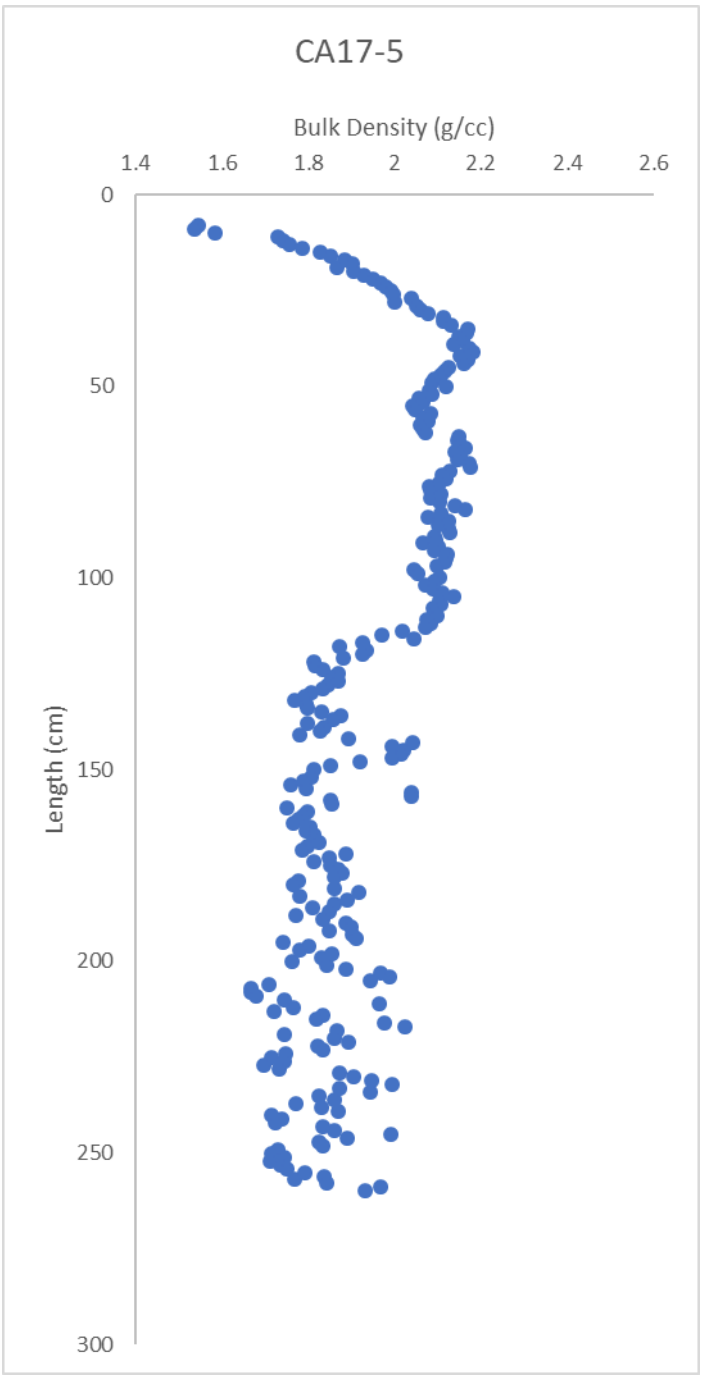

Figure A.4. Gamma derived bulk density plot for vibracore CA17-5

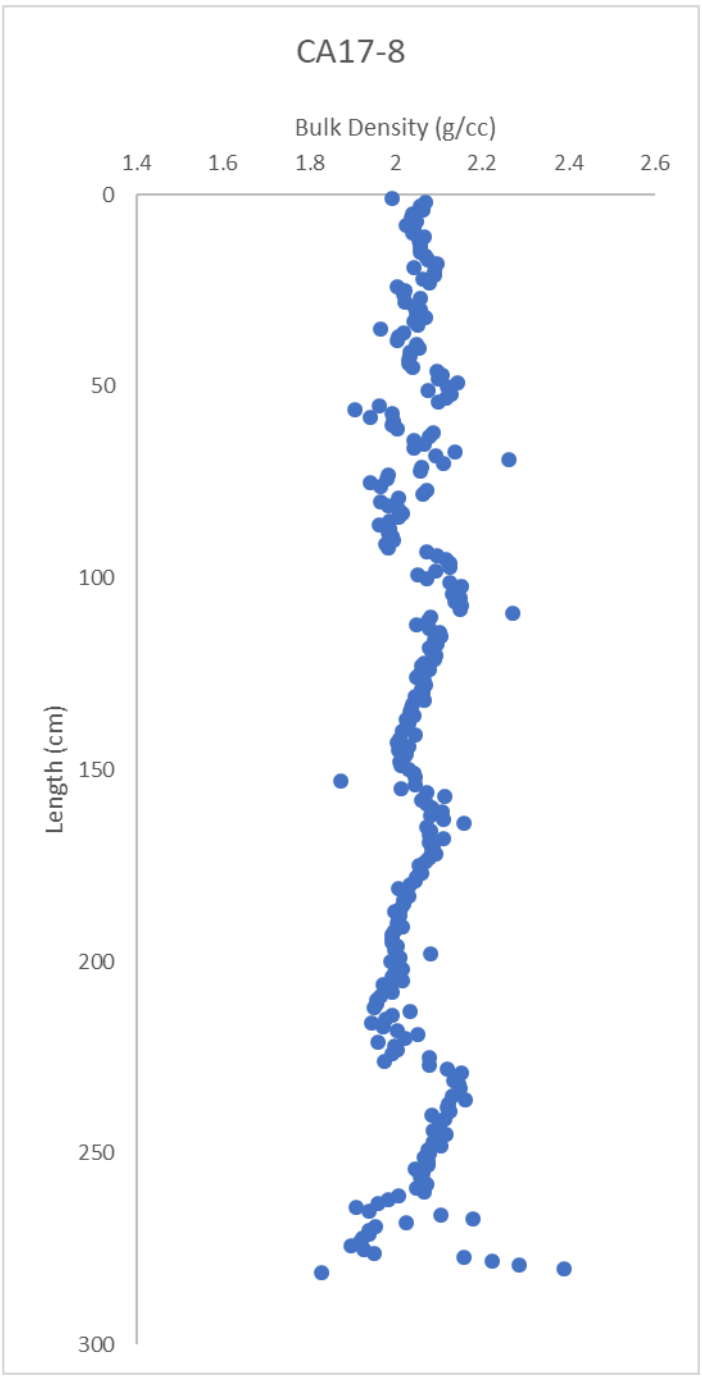

Figure A.5. Gamma derived bulk density plot for vibracore CA17-8

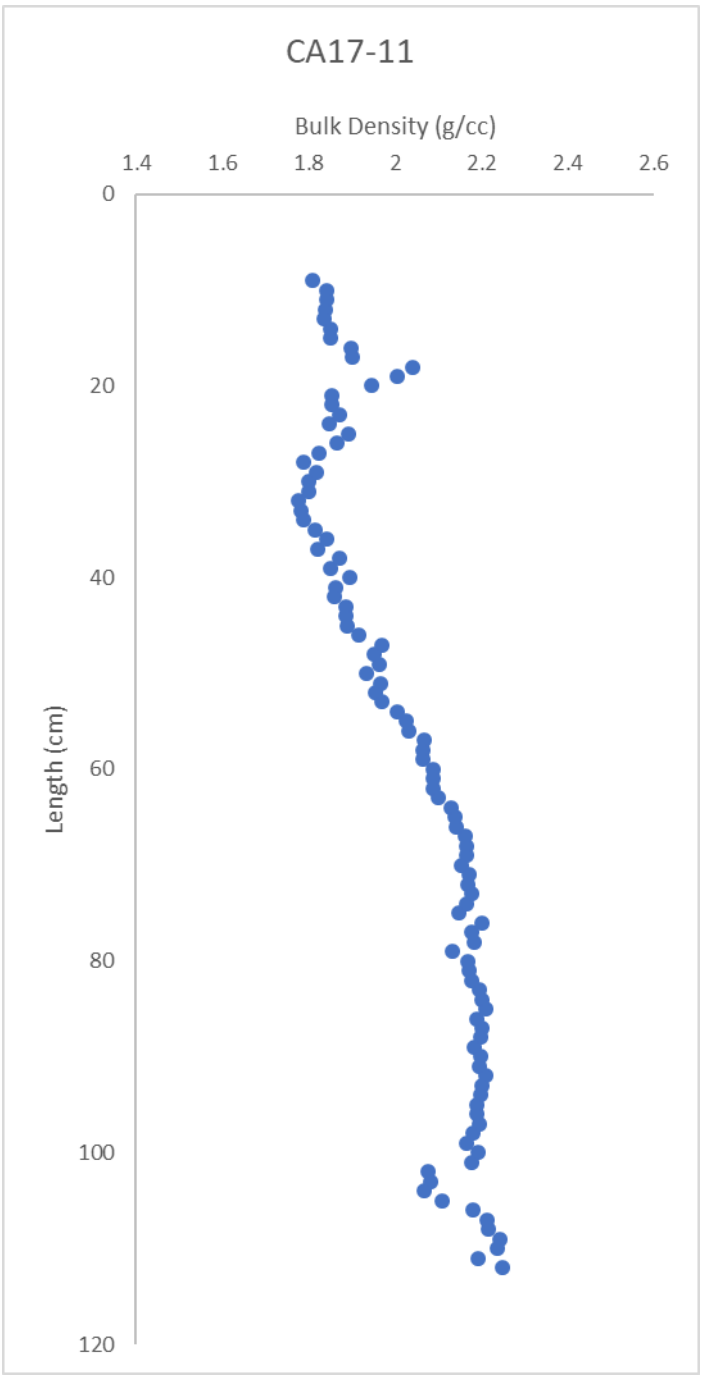

Figure A.6. Gamma derived bulk density plot for vibracore CA17-11

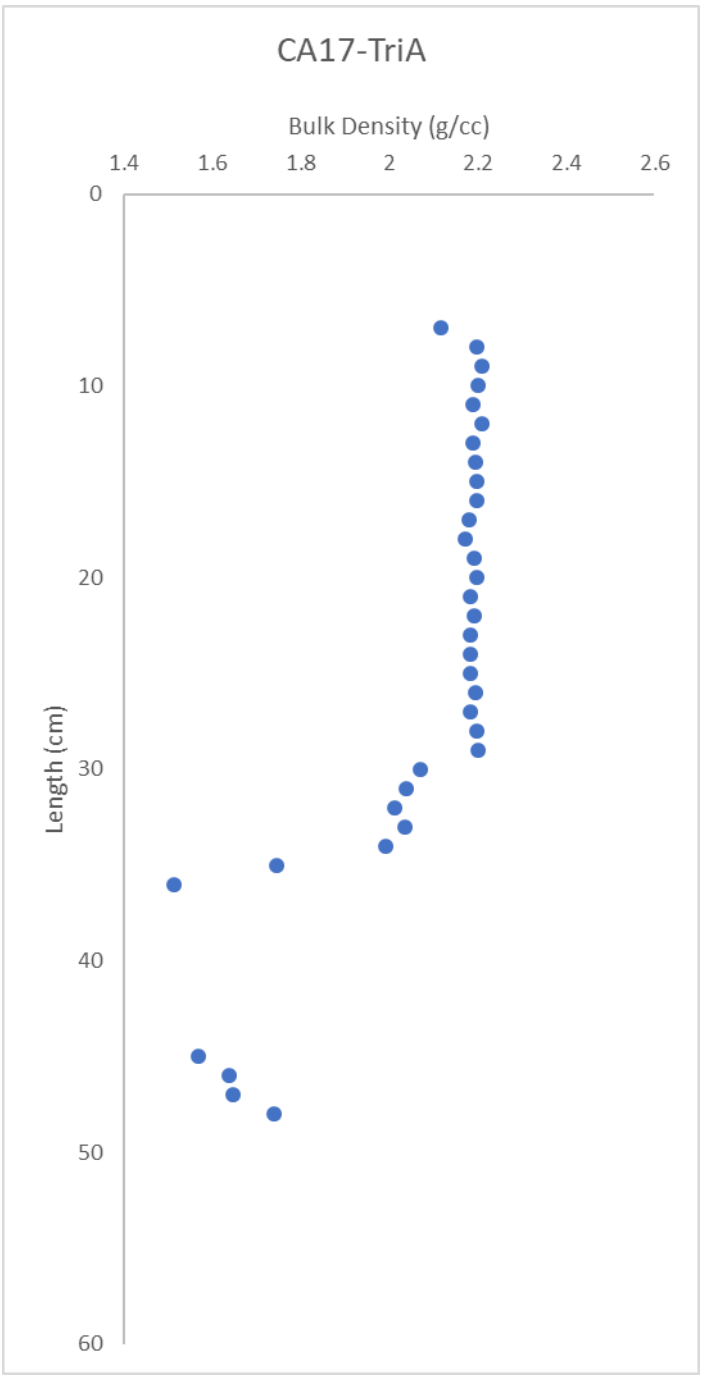

Figure A.7. Gamma derived bulk density plot for vibracore CA17-TriA

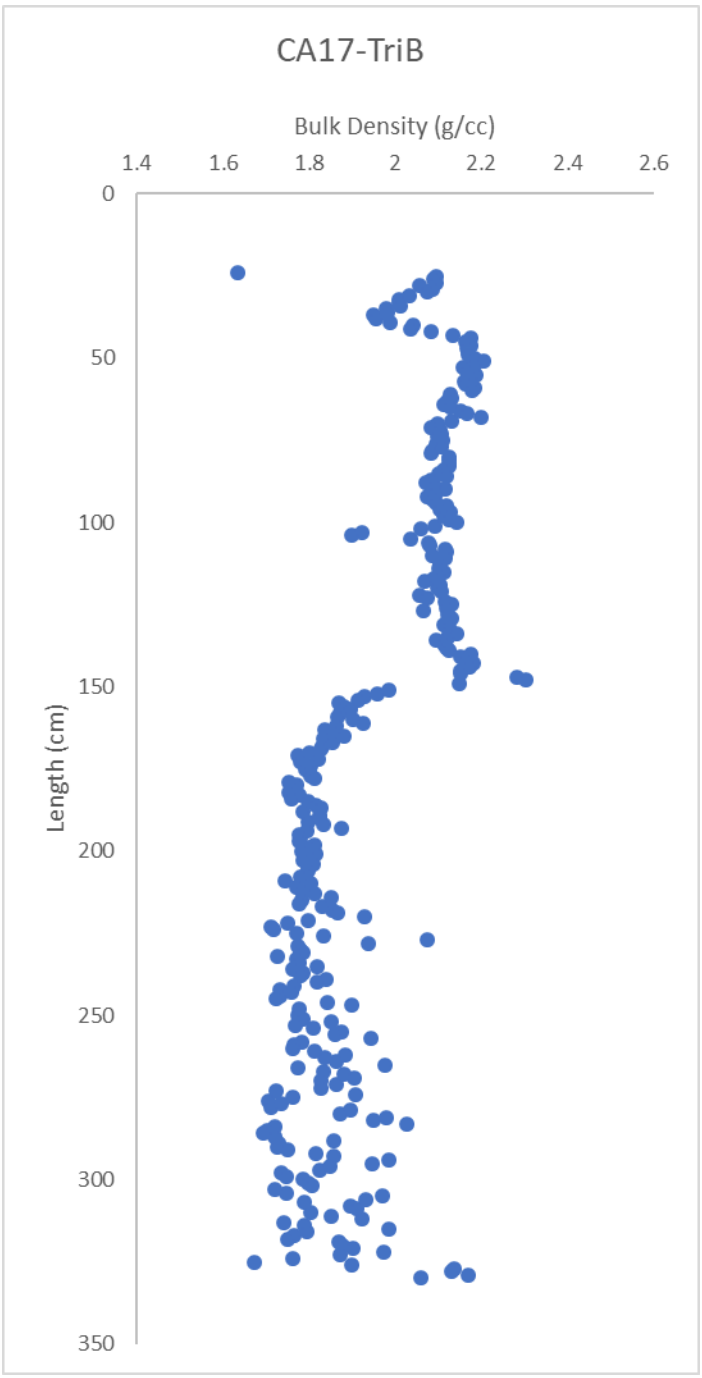

Figure A.8. Gamma derived bulk density plot for vibracore CA17-TriB

Appendix B. Grain Size

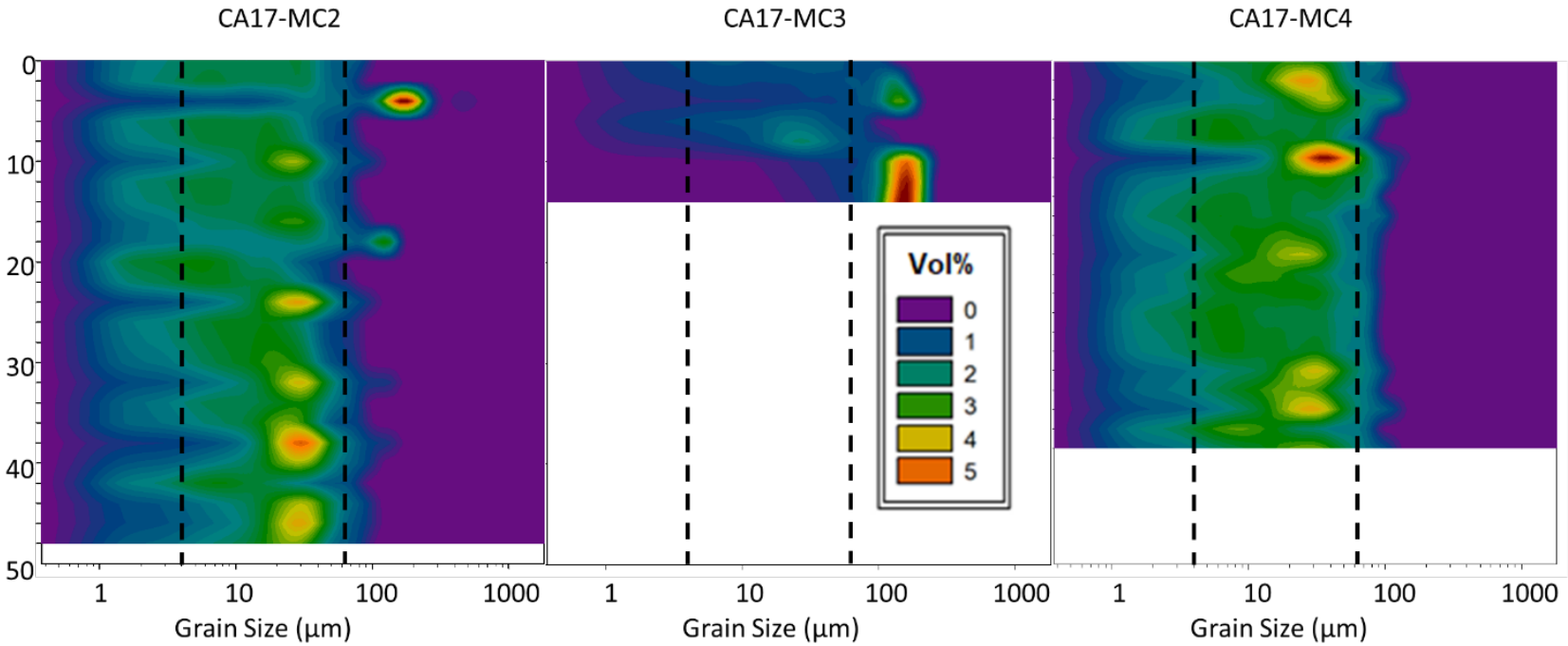

Figure B.1. Grain size contour plots for multicores CA17-MC2, CA17-MC3, and CA17-MC4.

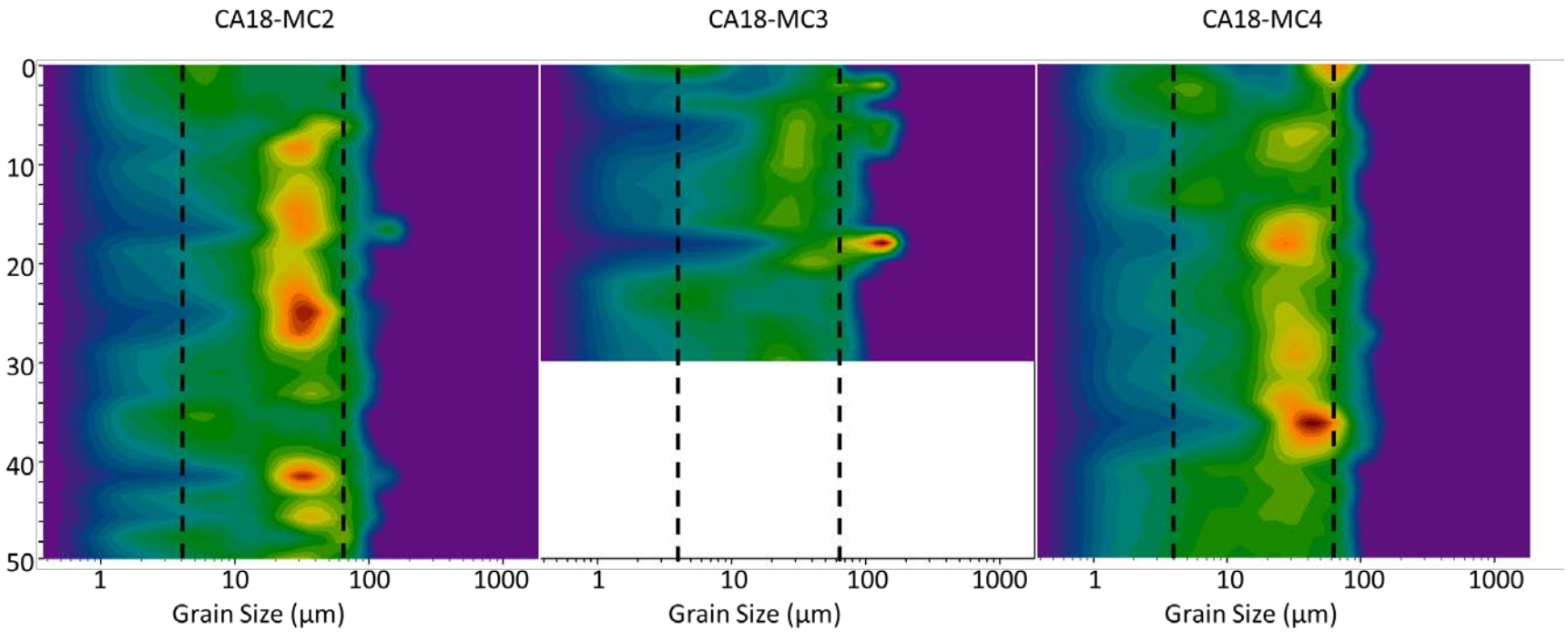

Figure B.2. Grain size contour plots for multicores CA18-MC2, CA18-MC3, and CA18-MC4.

CA17-MC5

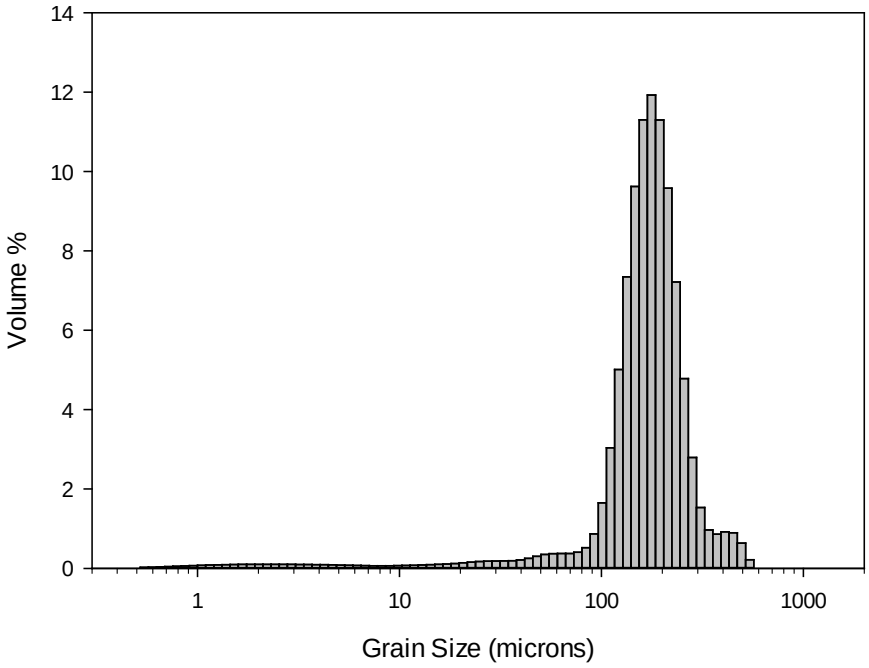

Figure B.3. Grain size histogram of CA17-MC5.

CA17-MC11

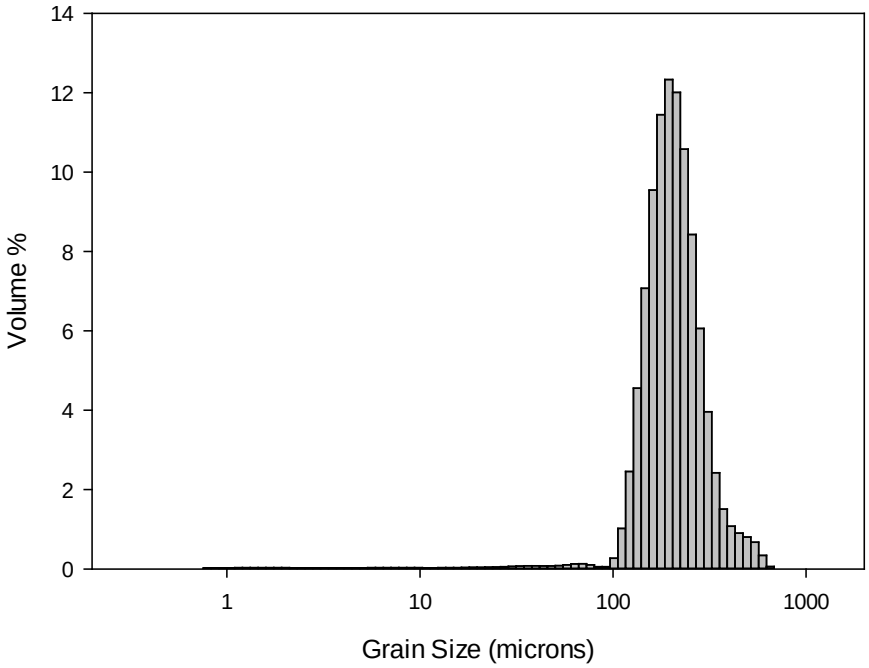

Figure B.4. Grain size histogram of CA17-MC11.

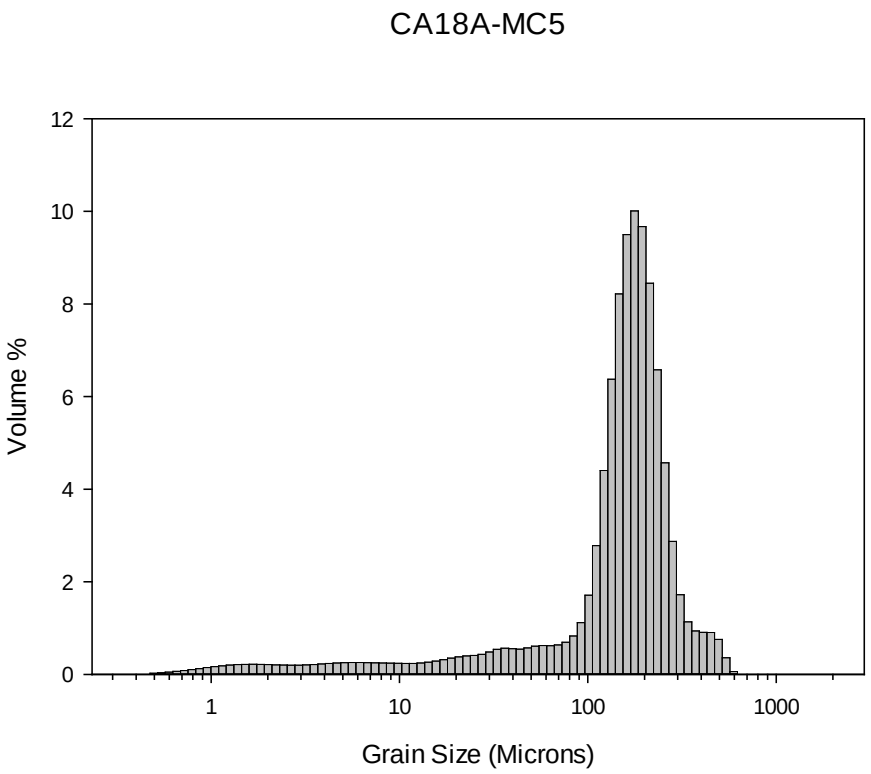

Figure B.5. Grain size histogram of CA18-MC5.

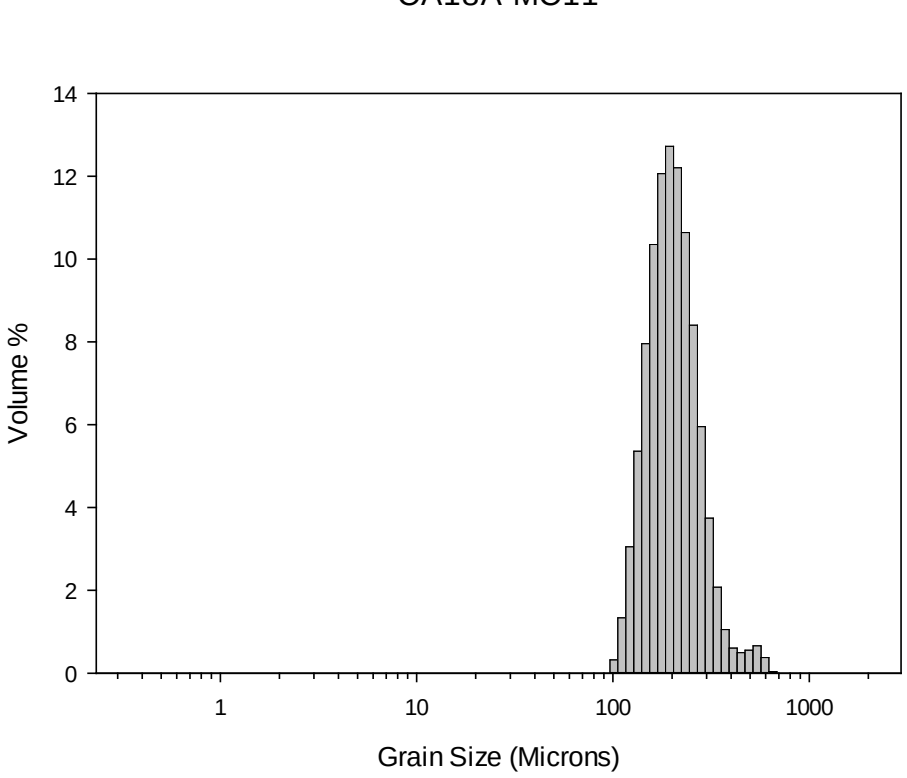

Figure B.6. Grain size histogram of CA18-MC11.

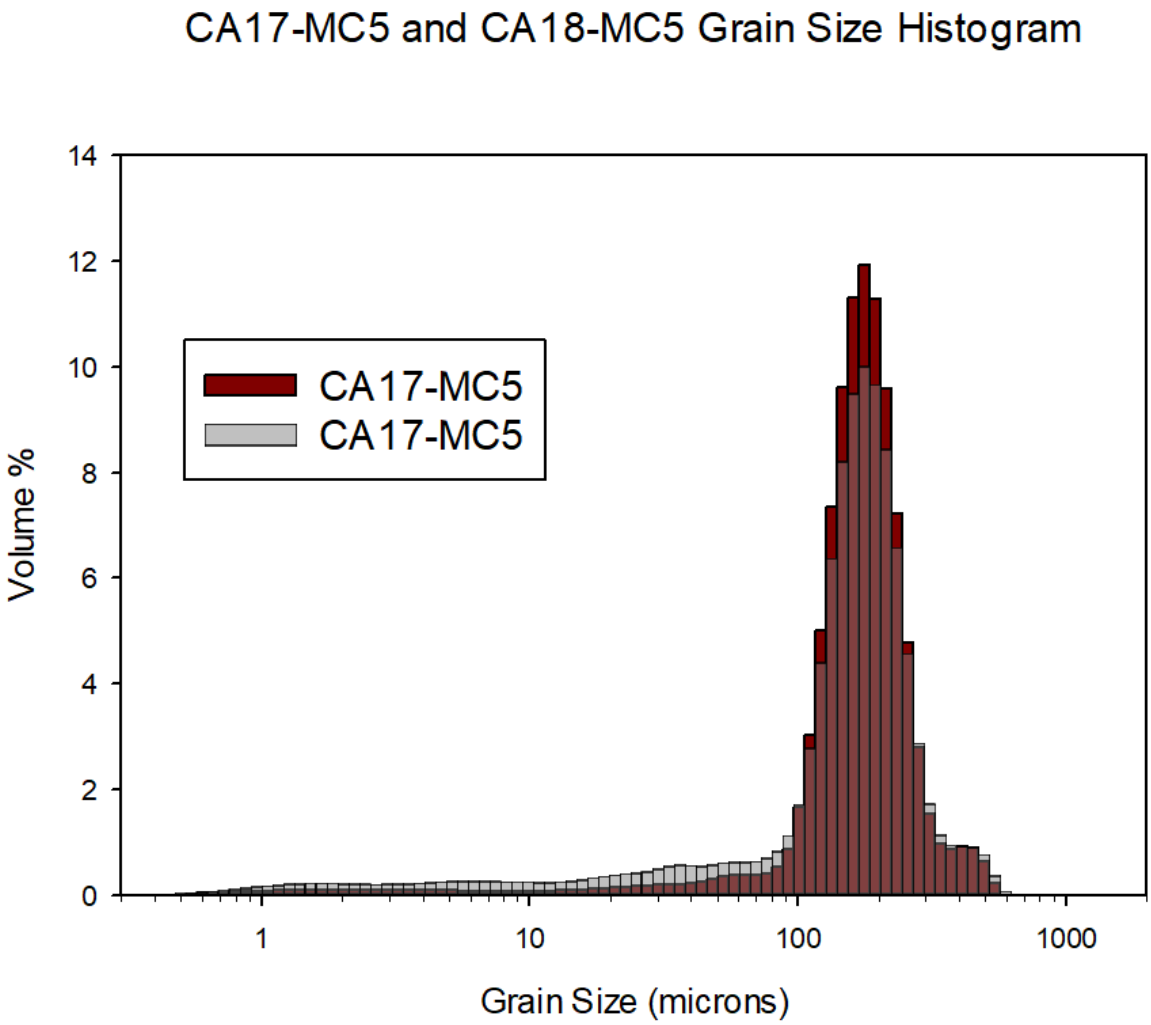

Figure B.7. Grain size histogram comparison of CA17-MC5 and CA18-MC5.

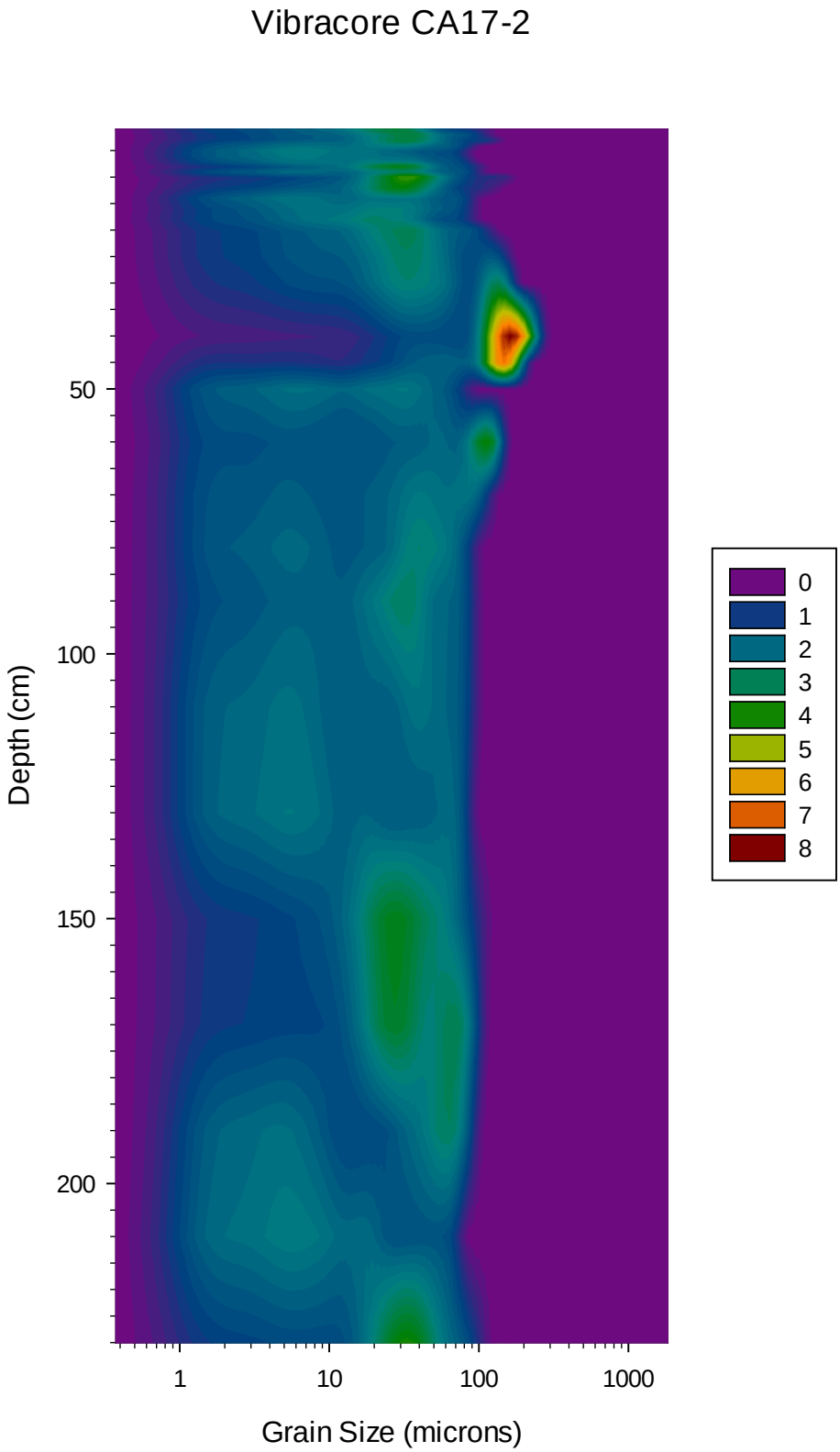

Figure B.8. Grain size contour plot of CA17-2.

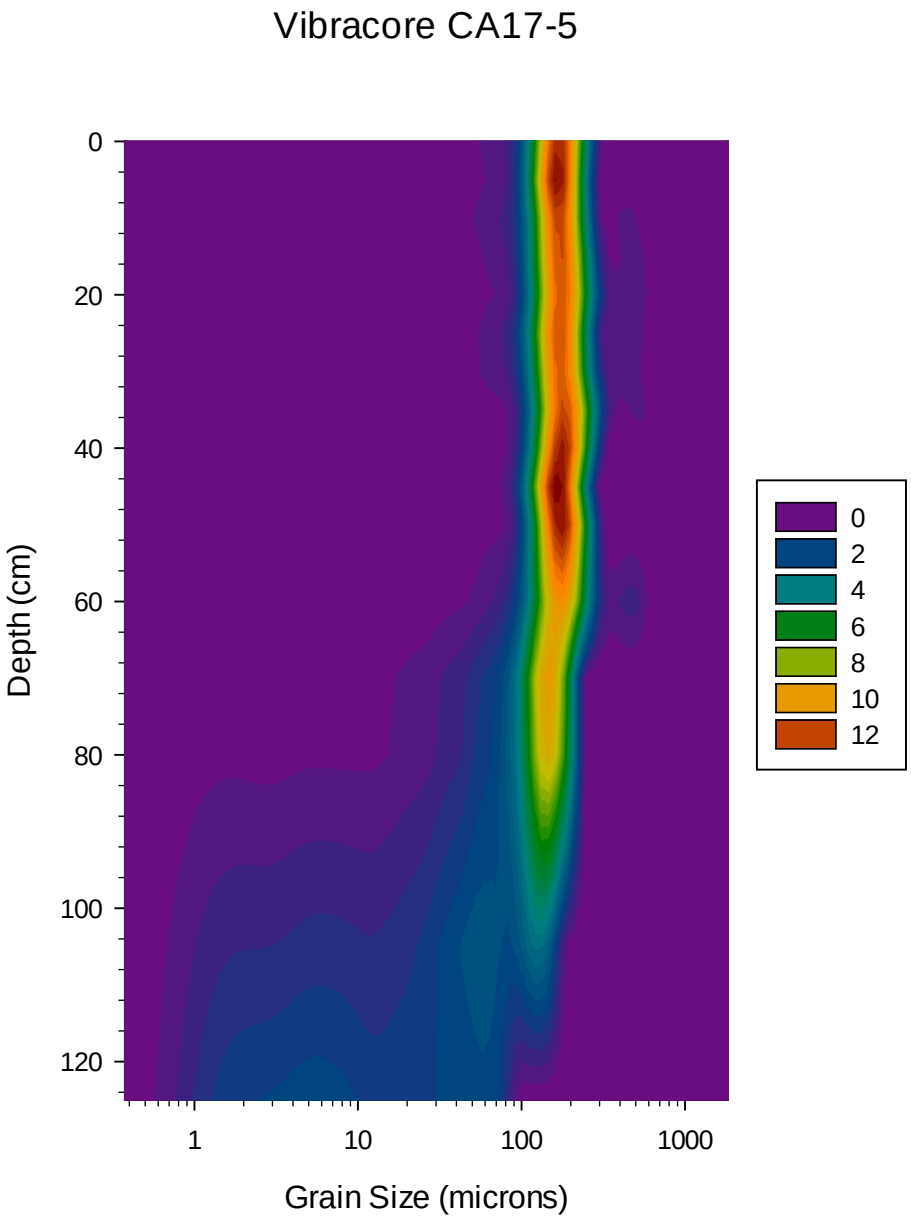

Figure B.9. Grain size contour plot of CA17-5.

Appendix C. Additional Core and ^{7}Be Data.

Table C.1. CA17-MC2 Beryllium Activity

Depth (cm)	^{7}Be Activity (dpm g^{-1})	Error (dpm g^{-1})
2	6.904181	0.532703
4	9.139494	0.696547
6	2.164558	0.362125
8	0	0
10	2.00861	0.492779
12	1.464089	0.493075
14	0	0

Table C.2. CA17-MC3 Beryllium Activity

Depth (cm)	^{7}Be Activity (dpm g^{-1})	Error (dpm g^{-1})
2	4.785301	0.685096
4	5.234192	0.826891
6	2.059832	0.573918
8	0.824333	0.585797
10	0	0
12	0	0

Table C.3. CA17-MC4 Beryllium Activity

Depth (cm)	^{7}Be Activity (dpm g^{-1})	Error (dpm g^{-1})
2	3.91679	0.536388
4	1.172877	0.457536
6	0	0

Table C.4. CA18-MC2 Beryllium Activity

Depth (cm)	^{7}Be Activity (dpm g^{-1})	Error (dpm g^{-1})
2	5.294772	0.870472
4	5.757441	0.777561
6	5.450311	0.832136
8	2.65962	0.685802
10	3.409095	0.842397
12	3.36173	0.754978
14	0.554869	0.637454
16	0	0

Table C.5. CA18-MC3 Beryllium Activity

Depth (cm)	^{7}Be Activity (dpm g^{-1})	Error (dpm g^{-1})
2	5.819709	0.68211
4	4.400279	0.524199
6	2.976853	0.541495
8	0.788503	0.342875
10	0	0

Table C.6. CA18-MC4 Beryllium Activity

Depth (cm)	^{7}Be Activity (dpm g^{-1})	Error (dpm g^{-1})
2	7.294679	0.706947
4	5.310429	0.588232
6	6.528747	0.708803
8	5.34241	0.722064
10	4.600186	0.78118
12	6.607954	0.790543
14	9.175468	1.00637
16	3.730696	0.733617
18	0	0

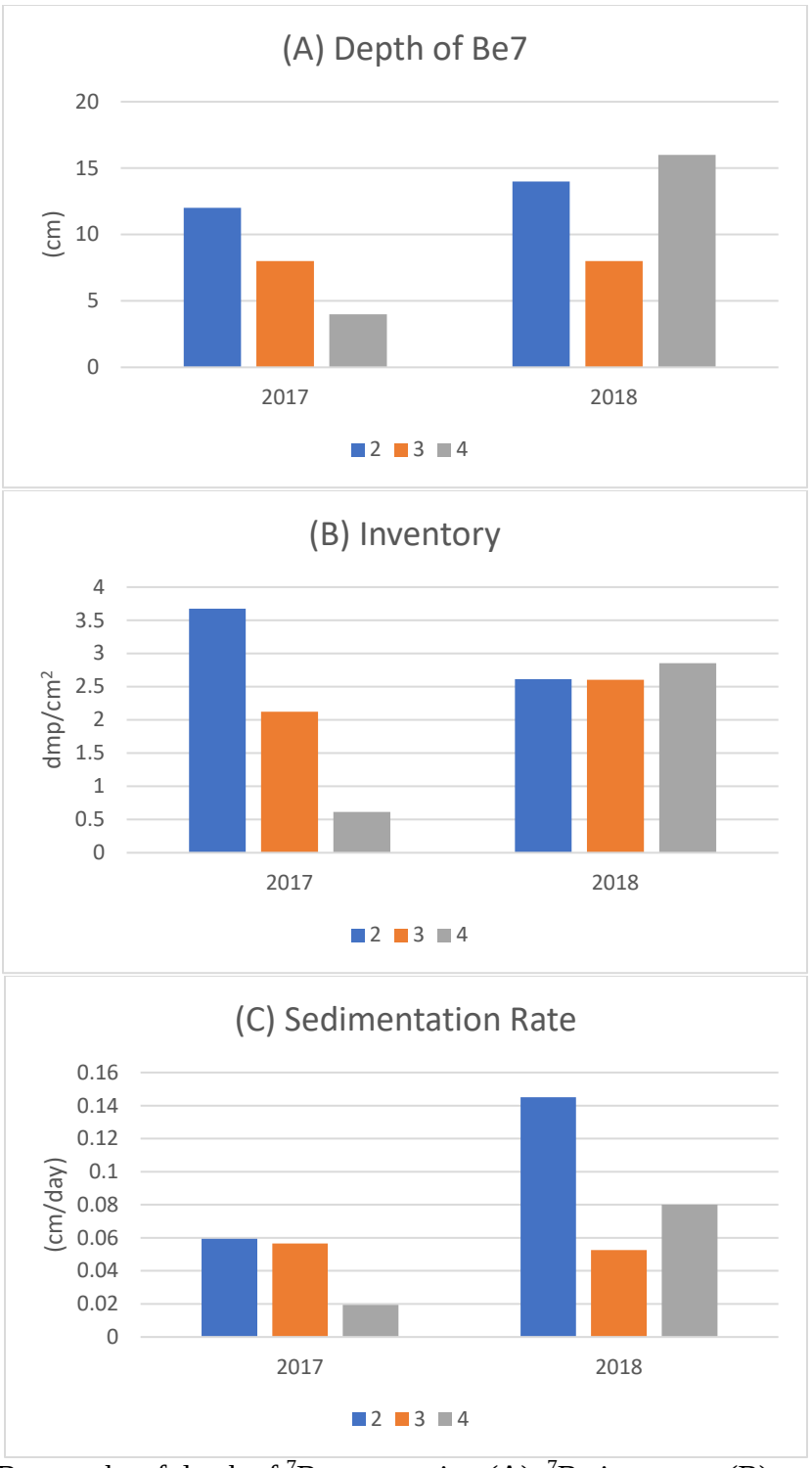

Figure C.1. Bar graphs of depth of ^{7}Be penetration (A), ^{7}Be inventory (B), and calculated sedimentation rates (C) from coring locations 2, 3, and 4 showing differences between 2017 and 2018.

Appendix D. Satellite Imagery

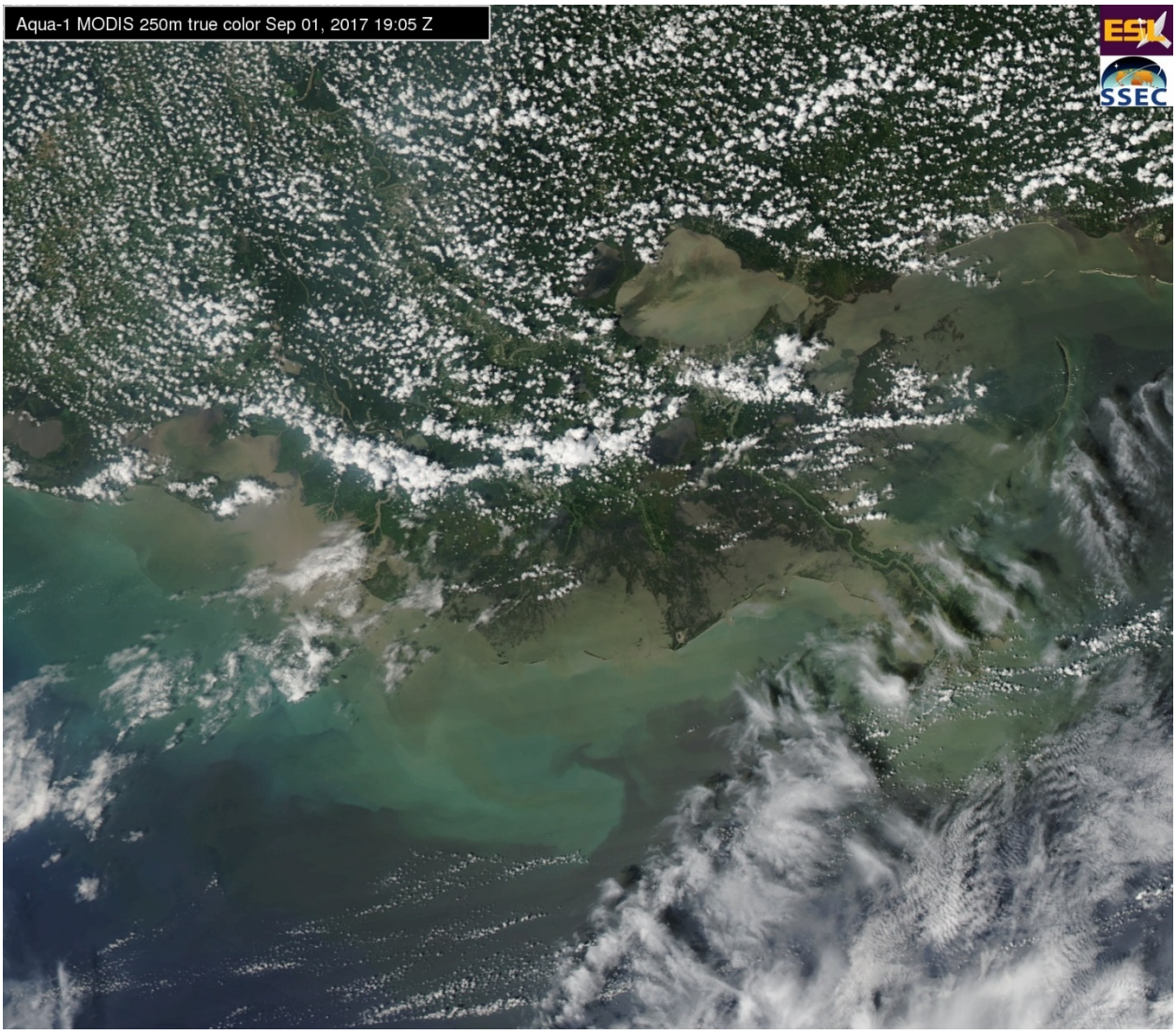

Figure D.1. MODIS satellite imagery of Hurricane Harvey on September 1, 2017.

Appendix E. X-ray Images

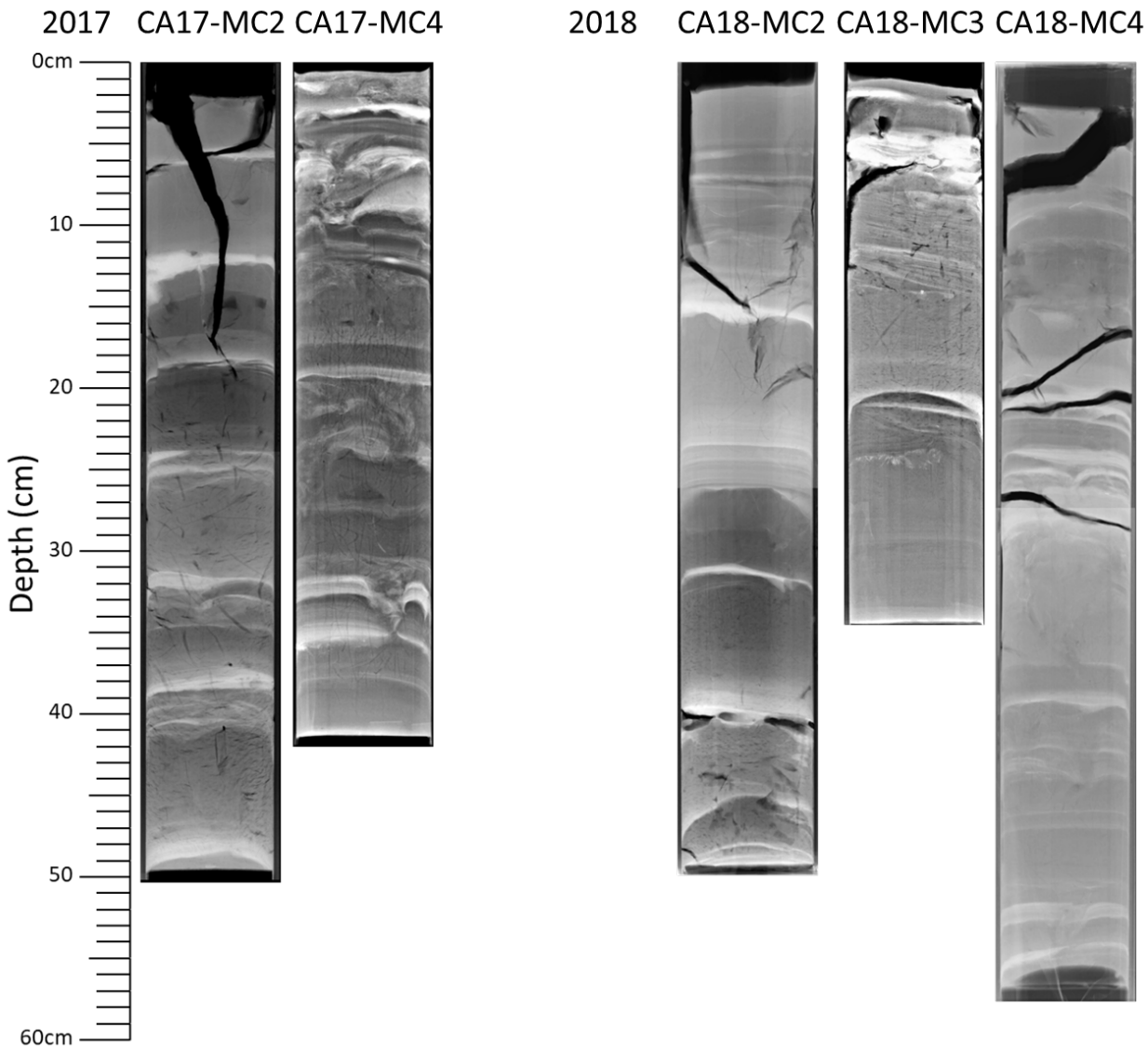

Figure E.1. X-ray images of multicores taken in 2017 and 2018.

References

Allison, M. A., Demas, C. R., Ebersole, B. A., Kleiss, B. A., Little, C. D., Meselhe, E. A., Powell, N. J., Pratt, T. C., and Vosburg, B. M., 2012, A water and sediment budget for the lower Mississippi–Atchafalaya River in flood years 2008–2010: Implications for sediment discharge to the oceans and coastal restoration in Louisiana: Journal of Hydrology, v. 432-433, p. 84-97.

Allison, M.A., Kineke, G.C., Gordon, E.S. and Goni, M.A., 2000. Development and reworking of a seasonal flood deposit on the inner continental shelf off the Atchafalaya River. Continental Shelf Research, 20(16), pp.2267-2294.

Baskaran, M., Coleman, C.H. and Santschi, P.H., 1993. Atmospheric depositional fluxes of 7Be and 210Pb at Galveston and College Station, Texas. Journal of Geophysical Research: Atmospheres, 98(D11), pp.20555-20571.

Baskaran, M., Ravichandran, M. and Bianchi, T.S., 1997. Cycling of7Be and210Pb in a High DOC, Shallow, Turbid Estuary of South-east Texas. Estuarine, Coastal and Shelf Science, 45(2), pp.165-176.

Bomer, E.J., Bentley, S.J., Hughes, J.E., Wilson, C.A., Crawford, F. and Xu, K., 2019. Deltaic morphodynamics and stratigraphic evolution of middle Barataria Bay and middle Breton sound regions, Louisiana, USA: Implications for River-Sediment Diversions. Estuarine, Coastal and Shelf Science, 224, pp.20-33.

Bouma, A.H., 1968. Distribution of minor structures in Gulf of Mexico sediments.

Bentley, S.J., Furukawa, Y. and Vaughan, W.C., 2000. Record of event sedimentation in Mississippi Sound.

Bentley, S.J., 2002. Dispersal of fine sediments from river to shelf: process and product.

Bentley, S.J., Keen, T.R., Blain, C.A. and Vaughan, W.C., 2002. The origin and preservation of a major hurricane event bed in the northern Gulf of Mexico: Hurricane Camille, 1969. Marine Geology, 186(3-4), pp.423-446.

Chamberlain, E.L., Törnqvist, T.E., Shen, Z., Mauz, B. and Wallinga, J., 2018. Anatomy of Mississippi Delta growth and its implications for coastal restoration. Science advances, 4(4), p.eaar4740.

Coastal Engineering Consultant Inc. 2017. Project Completion Report - Caminada Headland Beach and Dune Restoration Project, BA-45/BA-143.

Cobb, M., Keen, T.R. and Walker, N.D., 2008. Modeling the circulation of the Atchafalaya Bay system. Part 2: river plume dynamics during cold fronts. Journal of Coastal Research, pp.1048-1062.

Courtois, A, 2018. A Regional Survey of River-plume Sedimentation on the Mississippi River Delta Front. M.S. Thesis, Louisiana State University

Corbett, D.R., McKee, B. and Duncan, D., 2004. An evaluation of mobile mud dynamics in the Mississippi River deltaic region. Marine Geology, 209(1-4), pp.91-112.

CPRA (Coastal Protection and Restoration Authority), 2012. Louisiana's Comprehensive Master Plan for a Sustainable Coast. Baton Rouge, Louisiana: CPRA, 188p

CPRA (Coastal Protection and Restoration Authority), 2017. Caminada Headland Beach and Dune Restoration – Increment II (BA-143) Completion Report. Baton Rouge, Louisiana: CPRA, 187p

Denommee, K.C., Bentley, S.J., Harazim, D. and Macquaker, J.H., 2016. Hydrodynamic controls on muddy sedimentary-fabric development on the Southwest Louisiana subaqueous delta. Marine Geology, 382, pp.162-175.

DiMego, G.J., Bosart, L.F. and Endersen, G.W., 1976. An examination of the frequency and mean conditions surrounding frontal incursions into the Gulf of Mexico and Caribbean Sea. Monthly Weather Review, 104(6), pp.709-718.

Frazier DE 1967 Recent deltaic deposits of the Mississippi River: their development and chronology. Trans Gulf Coast Assoc Geol Soc 17:287–315

Geotek Ltd. 2018. Gamma Dsensity. Retrieved Oct 05, 2018, from https://www.geotek.co.uk/sensors/gammadensity/

Goni, M.A., Alleau, Y., Corbett, R., Walsh, J.P., Mallinson, D., Allison, M.A., Gordon, E., Petsch, S. and Dellapenna, T.M., 2007. The effects of Hurricanes Katrina and Rita on the seabed of the Louisiana shelf. The Sedimentary Record, 5(1), pp.4-9.

Keller, G., Bentley, S.J., Xu, K., Maloney, J., Miner, M., Georgiou, I., 2016, River-plume sedimentation and 210Pb/7Be seabed delivery on the Mississippi River delta front. Geo Marine Letters doi:10.1007/s00367-016-0476-0.

Khalil, S.M., Finkl, C.W., Andrews, J. and Knotts, C.P., 2007. Restoration-quality sand from Ship Shoal, Louisiana: geotechnical investigation for sand on a drowned barrier island. In Coastal Sediments' 07 (pp. 685-698).

Khalil, S.M., Knotts, C.P. and Tate, B., 2007. Restoration of Louisiana barrier islands: engineering approaches to hazard mitigation by modulating coastal environments. In Coastal Engineering 2006: (In 5 Volumes) (pp. 1951-1963).

Kindinger, J., Flocks, J., Kulp, M., Penland, S., Britsch, L.D., Brewer, G., Brooks, G.L., Dadisman, S., Dreher, C. and Ferina, N., 2001. Sand resources, regional geology, and coastal processes for the restoration of the Barataria barrier shoreline (No. 2001-384).

Kulp, M., Penland, S., Williams, S.J., Jenkins, C., Flocks, J. and Kindinger, J., 2005. Geologic framework, evolution, and sediment resources for restoration of the Louisiana coastal zone. Journal of coastal research, pp.56-71.

Liu, H., Xu, K., Bentley, S.J., Wilson, C., Xue, Z., Miner, M.D., 2018. Sediment transport and geomorphologic response in multiple dredge pits near Ship Shoal of coastal Louisiana. AGU Fall Meeting, Washington, DC, 10-14 December. Poster.

Liu, H., Xu, K.H., Li, B., Han, Y., Li, G., 2019 Sediment Identification Using Machine Learning Classifiers in a Mixed-Texture Dredge Pit of Louisiana Shelf for Coastal Restoration. Water, 11, 1257. https://www.mdpi.com/2073-4441/11/6/1257.

Maloney, J.M., Bentley, S.J., Xu, K., Obelcz, J., Georgiou, I.Y. and Miner, M.D., 2018. Mississippi River subaqueous delta is entering a stage of retrogradation. Marine Geology, 400, pp.12-23.

Moeller, C.C., Huh, O.K., Roberts, H.H., Gumley, L.E. and Menzel, W.P., 1993. Response of Louisiana coastal environments to a cold front passage. Journal of Coastal Research, pp.434-447.

Mossa, J. and Roberts, H.H., 1990. Synergism of riverine and winter storm-related sediment transport processes in Louisiana's coastal wetlands.

Motti, J. and Kulp, M.A., 2003. Descriptive Logs and Textural Analysis Data for BSS2000 Vibracores: Ship Shoal Area. New Orleans, Louisiana: Louisiana Department of Natural Resources, 15p.

Muhammad, Z., Bentley, S. J., Febo, L. A., Droxler, A. W., Dickens, G. R., Peterson, L. C., and Opdyke, B. N., 2008, Excess 210Pb inventories and fluxes along the continental slope and basins of the Gulf of Papua: Journal of Geophysical Research: Earth Surface (2003–2012), v. 113, no. F1.

Murray, S.P., 1998. An observational study of the Mississippi-Atchafalaya coastal plume.

Nairn, R., Johnson, J.A., Hardin, D. and Michel, J., 2004. A biological and physical monitoring program to evaluate long-term impacts from sand dredging operations in the United States outer continental shelf. Journal of Coastal Research, pp.126-137.

Nairn, R., Q. Lu and S. Langendyk 2005. A study to address the issue of seafloor stability and the Impact on Oil and Gas infrastructure in the Gulf of Mexico. US Dept. of the Interior, MMS, Gulf of Mexico OCS Region, New Orleans, LA OCS Study MMS 43: 179.

Nittrouer, JA, Allison, MA, Campanella, R, 2008. Bedform transport rates for the lowermost Mississippi River. J Geophys Res Earth Surf (2003-2012) 113:F03004. doi: 10.1029/2007JF000795.

Obelcz, J., Xu, K.H., Bentley, S.J., Li, C., Miner, M.D., O'Connor, M., Wang, J., 2016. Evolution of Mud-capped Dredge Pits following Excavation: Sediment Trapping and Slope Instability, AGU Ocean Sciences Meeting, New Orleans, Louisiana.

O'Connor, M., 2017. Sediment Infilling of Louisiana Continental-shelf Dredge Pits: A Record of Sedimentary Processes in The Northern Gulf of Mexico. M.S. Thesis, Louisiana State University, 68pg.

Penland, S., Boyd, R. and Suter, J.R., 1988. Transgressive depositional systems of the Mississippi delta plain: a model for barrier shoreline and shelf sand development. Journal of Sedimentary Research, 58(6), pp.932-949.

Penland, S., Connor, P.F., Jr., Beall, A., Fearnley, S. and Williams, S.J. 2005. Changes in Louisiana's Shoreline: 1855-2002. In: Finkl, C.W. and Khalil, S.M., (eds.), Savings America's Wetland: Strategies for Restoration of Louisiana's Coastal Wetlands and Barrier Islands, Journal of Coastal Research, Special Issue No. 44, 7-39.

Penland, S., Suter, J.R. and Moslow, T.F., 1986. Inner-shelf shoal sedimentary facies and sequences: Ship Shoal, northern Gulf of Mexico.

Penland, S. and Ramsey, K.E., 1990. Relative sea-level rise in Louisiana and the Gulf of Mexico: 1908-1988. Journal of Coastal Research, pp.323-342.

Perez, B.C., Day Jr, J.W., Rouse, L.J., Shaw, R.F. and Wang, M., 2000. Influence of Atchafalaya River discharge and winter frontal passage on suspended sediment concentration and flux in Fourleague Bay, Louisiana. Estuarine, Coastal and Shelf Science, 50(2), pp.271-290.

Restreppo, G.A., Bentley, S.J., Wang, J. and Xu, K., 2019. Riverine Sediment Contribution to Distal Deltaic Wetlands: Fourleague Bay, LA. Estuaries and Coasts, 42(1), pp.55-67.

Roberts, H.H., 1997. Dynamic changes of the Holocene Mississippi River delta plain: the delta cycle. Journal of Coastal Research, pp.605-627.

Rotondo, K.A., and S.J. Bentley. 2003. Deposition and resuspension of fluid muds on the western Louisiana inner continental shelf. Gulf Coast Association of Geological Societies Transactions 53: 722–731.

Stone, G.W., Condrey, R.E., Fleeger, J.W., Khalil, S.M., Kobashi, D., Jose, F., Evers, E., Dubois, S., Liu, B., Arndt, S. and Gelpi, C., 2009. Environmental investigation of long-term use of Ship Shoal sand resources for large scale beach and coastal restoration in Louisiana. US Dept. of the Interior, Minerals Management Service, Gulf of Mexico OCS Region, New Orleans, LA. OCS Study MMS, 24, p.278.

Stone, G.W. and McBride, R.A., 1998. Louisiana Barrier Islands and Their Importance in Wetland Protection: Forecasting Shoreline Change and Subsequent Response of Wave Climate. Journal of Coastal Research, pp.900-915.

Stone, G.W., Pepper, D.A., Xu, J. and Zhang, X., 2004. Ship Shoal as a Prospective Borrow site for barrier island restoration, Coastal south-central Louisiana, USA: Numerical wave modeling and field measurements of hydrodynamics and sediment transport. Journal of Coastal Research, pp.70-88.

Sommerfield, C.K., Nittrouer, C.A. and Alexander, C.R., 1999. 7Be as a tracer of flood sedimentation on the northern California continental margin. Continental Shelf Research, 19(3), pp.335-361.

Törnqvist, T.E., Kidder, T.R., Autin, W.J., van der Borg, K., de Jong, A.F., Klerks, C.J., Snijders, E.M., Storms, J.E., van Dam, R.L. and Wiemann, M.C., 1996. A revised chronology for Mississippi River subdeltas. Science, 273(5282), pp.1693-1696.

Van Heerden, I.L. and DeRouen Jr, K., 1997. Implementing a barrier island and barrier shoreline restoration program: The state of Louisiana's perspective. Journal of Coastal Research, pp.679-685.

Walker, N.D., 1996. Satellite assessment of Mississippi River plume variability: causes and predictability. Remote sensing of environment, 58(1), pp.21-35.

Walker, N.D. and Hammack, A.B., 2000. Impacts of winter storms on circulation and sediment transport: Atchafalaya-Vermilion Bay region, Louisiana, USA. Journal of Coastal Research, pp.996-1010.

Wang, J., Xu, K., Li, C. and Obelcz, J., 2018. Forces Driving the Morphological Evolution of a Mud-Capped Dredge Pit, Northern Gulf of Mexico. Water, 10(8), p.1001.

Wells, J.T. and Kemp, G.P., 1981. Atchafalaya mud stream and recent mudflat progradation: Louisiana chenier plain.

Williams, S Jeffress & Kulp, Mark & Penland, S & Kindinger, Jack & Flocks, James. (2011). Mississippi River delta plain, Louisiana coast, and inner shelf Holocene geologic framework, processes, and resources. Gulf of Mexico Origin, Waters, and Biota: Volume III, Geology. 175-193.

Wright, L.D., Sherwood, C.R. and Sternberg, R.W., 1997. Field measurements of fairweather bottom boundary layer processes and sediment suspension on the Louisiana inner continental shelf. Marine Geology, 140(3-4), pp.329-345.

Wright, L.D., Friedrichs, C.T., Kim, S.C. and Scully, M.E., 2001. Effects of ambient currents and waves on gravity-driven sediment transport on continental shelves. Marine Geology, 175(1-4), pp.25-45.

Xu, K., Bentley, S., Robichaux, P., Sha, X. and Yang, H., 2016. Implications of texture and erodibility for sediment retention in receiving basins of coastal Louisiana diversions. Water, 8(1), p.26.

Xu, K., Harris, C.K., Hetland, R.D. and Kaihatu, J.M., 2011. Dispersal of Mississippi and Atchafalaya sediment on the Texas–Louisiana shelf: Model estimates for the year 1993. Continental Shelf Research, 31(15), pp.1558-1575.

Xu, K., Mickey, R.C., Chen, Q., Harris, C.K., Hetland, R.D., Hu, K. and Wang, J., 2016. Shelf sediment transport during hurricanes Katrina and Rita. Computers & Geosciences, 90, pp.24-39.

Xu, K.H., Obelcz, J., Bentley, S.J., Miner, M.D., Li, C., Chaichitehrani, N., O'Connor, M., Wang, J., 2016. Assessment of Mud-Capped Dredge Pit Evolution Offshore Louisiana: Implications to Sand Excavation and Coastal Restoration, AGU Ocean Sciences Meeting, New Orleans, Louisiana.

Zang, Z., Xue, Z.G., Xu, K., Bentley, S.J., Chen, Q., D'Sa, E.J. and Ge, Q., 2019. A Two Decadal (1993–2012) Numerical Assessment of Sediment Dynamics in the Northern Gulf of Mexico. Water, 11(5), p.938.

Vita

Zehao Xue was born in China and grew up in Waterloo, Canada. He received his B.S. in Geology from the University of Texas at Austin in 2017. In his undergraduate research on the Wax Lake Delta in Louisiana, Zehao developed an interest in coastal sedimentary processes. Following graduation, he came to Louisiana State University to work with Dr. Carol Wilson on sedimentation of Ship Shoal Borrow Area for coastal restoration research.